A STUDY OF GAMMA RAY TOTAL ATTENUATION AND PHOTO ABSORPTION COEFFICIENT IN DIFFERENT ELEMENTS

By
Dilbetigle Assefa

A THESIS PRESENTED TO
THE SCHOOL OF GRADUATE STUDIES
ADDIS ABABA UNIVERSITY
IN PARTIAL FULFILLMENT OF THE REQUIREMENTS
FOR THE DEGREE OF

MASTER OF SCIENCE in PHYSICS

ADDIS ABABA, ETHIOPIA
AUGUST 2006

ADDIS ABABA UNIVERSITY

DEAPRMENT OF PHYSICS

The undersigned hereby certify that they have read and recommend to the Faculty of Science for acceptance a senior project entitled "**A study of gamma ray total attenuation and photo absorption coefficient in different elements**" by **Dilbetigle Assefa Master of Science**.

Dated: August 2006

Supervisor: _____
A.K. Chaubay (Professor)

Readers: _____
Dr.Tilahume Tesfaye

_____

ADDIS ABABA UNIVERSITY

Date: **August 2006**

Author: **Dilbetigle Assefa**

Title: **A study of gamma ray total attenuation and photo absorption coefficient in different elements**

Department: **Deaprment of Physics**

Degree: **M.Sc.** Convocation: **July** Year: **2006**

_____

Signature of Author

This Work is Dedicated to
My mother and my Grand mother

Table of Contents

List of Tables

List of Figures

Acknowledgements

First of all, I would like to express my sincere thanks to my adviser and instructor prof.A.K Chaubay for his effort in giving and supervising this work possible. I am also very grateful to him for making most of reference available and for introducing me to the subject.

I would like to thank the physics department of AAU for providing the necessary material for this work and the staff members especially for W/O Tsilat Adinew. I wish to express my gratitude to Dr.Tilahun Tesfaye for facilitating my work. And for Ato Zelalem Belayneh for technical support and encouragement throughout my work.

Furthermore, I would like to extend my warmest gratitude to my brother, sisters and friend Tesfaye neway for their consistent encouragement and support through out the study program.

Last but not least, I wish to thank to all my friends for their material and moral support.

Addis Ababa University Dilbetgle Assefa

June, 2006

Abstract

The study intends to measure the transmission of gamma rays such as ^{137}Cs, through Aluminium, Iron, Nickel, Copper, Tin, and lead absorbers using gamma ray spectroscopy techniques. Electrical pulses, carrying the physical information is displayed on the computer screen with the number of channels on the horizontal scale and number of pulses on the vertical scale. The multichannel Analyzer will then process there pulses, which are digitized.

The total linear attenuation coefficient (μ) of 662Kev gamma rays have been measured in the extended media of six elements under different geometry condition and using HPGe and NaI(Tl) detectors. Better result of total linear attenuation coefficient is obtained when an absorber near to a detector and using HPGe detector. This is due to the decreases in the exposure of the detector to the beams of gamma rays and high resolution power of HPGe detector respectively.

It also aims to determine the total linear attenuation coefficients for Tin using the energy of photons 122kev, 662kev, 1172kev, and 1332kev and to evaluate how it varies as a function of gamma rays energy. The result generally agree with theoretical calculations. Some discrepancies can be explained by the collimation, media and geometry of absorber. The dependence of cross-section on the atomic number and the energies of gamma ray is also seen due to the increases of binding energy and penetration power of gamma ray.

Introduction

The knowledge of the absorption properties of gamma rays is an important property of matter in many applicable area of science and Engineering. It is necessary in the treatment of shielding problem,testing of material, oil-well logging, quantitative measurements of tracers where the active substance can not be separated, as in biological or medical measurement in vivo, and finally for the determination of gamma-ray energies, either to identify a radioisotope or to establish a decay scheme. There is an important parameters for characterizing the penetration and diffusion of gamma rays in a medium which is known as attenuation coefficient. This parameter mainly depends on the photo energy and nature of medium. Several workers have conducted the systematic studies of attenuation coefficient using narrow beam geometry from time to time. **?**

This work is done with intention of showing, experimentally the dependence of total linear attenuation and photo absorption coefficients of copper, iron, nickel, lead, and tin on the atomic number, energy of gamma -rays and the geometry of the absorber respect to the source and detector. Using a gamma source of ^{137}Cs,^{60}Co,and ^{57}Co. Furthermore, it has been tried to obtain accurate measurement of the total linear attenuation and photo absorption coefficient for those elements by collimating the beam properly. When the transmitted beam is collimated properly. i.e, when narrow beam geometry is made, then the multiple scattered photons are prevented from reaching the detector. But as the collimator size and sample thickness are increased, the probability of multiple scattered photons to reach the detector increase. So, along with the uncollided photons the multiple scattered photons are also measured. This is because firstly with increase in sample thickness, more number of scattered photons are generated and secondly with increase in collimator size (half acceptance angle) the detector is exposed more to the scattered radiations. **?**

In this regard Gopal and Sanjeevaiah **?** have studied the effect of sample thickness on the measured attenuation coefficients of elements, Al, C, Cu, Sn, and Pb for 662kev gamma rays and reported that measured attenuation coefficient μ remains fairly constant for values of $\mu t < 1$, where t is the sample thickness.

In this thesis report, the first chapter deals the theory of radioactivity and the a decay of radionuclide, and more emphasized on gamma decay is given. A survey on features of interaction of gamma-radiation with matter, which encompasses the *photo electric* effect, the *compton effect*, and the *pair -production* properties of gamma -rays interaction. The working principle of sodium iodide, Ge(Li) and Ge detectors are described in Chapter 3. In Chapter 4 and 5 the main physical features of the experimental instruments and methods used in experiment are discussed. This measured data of Chapter 5 are treated using a comparative counting method to determine the the total attenuation and photo absorption of coefficient of those elements.

To improve the accuracy in the measurements of attenuation coefficient is very important, an attempt has been made in the present work to measure and study the effect of atomic number of the elements, energy of gamma -ray and the source, absorber and detector geometry on the measured total attenuation and photo absorption coefficient for the six elements.

Chapter 1

Radioactive Nuclei

1.1 Introduction

Historically radioactivity and hence the existence of the nucleus, were discovered as a consequence of apparently incomprehensible experimental observations. Becquerel placed a piece of mineral containing uranium on an unexposed photographic plate wrapped in black paper. Some days later he found that the pale was clouded as if it had been exposed to light, in spite of the fact that the black paper was completely opaque. Becquerel was at the time looking for a phenomenon of remission of light called fluorescence. He had discovered something very different, and his genius lay in the fact that he realized this. He showed subsequently that the radiation which was affecting the photographic plate depended neither on the particular chemical compound used(provided it contained uranium)nor on its temperature or other external circumstances. Then pierre and Marie curi isolated from uranium ore two elements hitherto unknown-polonium and radium-which were far more active than uranium. They showed that the radiation was a property of the atoms themselves, and that it was capable of ionizing gases, that is, of creating electric charges in an enclosed volume of gas, so that the latter become a conductor of electricity-a phenomenon previously observed in connection with the x-rays discovered by Roentgen. More surprisingly, this radiation carried with it a great deal of energy, since in spite of the very small quantities of emitting matter, it produced an observable heating effect in anything that absorbed it.

Next, Rutherford demonstrated that there were three types of ”rays” emitted by radium and its derivatives.These are alpha, beta, and gamma rays. **?**

1.2 Radioactive Decay

Activity of a radioisotope measures the source disintegration rate, which is not synonymous with the emission rate of radiation produced in its decay. Frequently, a given radiation will be emitted in only a fraction of all the decays. So a knowledge of the decay schema of the particulars isotope is necessary to infer a radiation emission rate from it activity. Also, the decay of a given radioisotope may lead to a daughter product whose activity also contributes to the radiation yield from the source. **?**

The activity of a radioisotope source is defined as its rate of decay and is given by the fundamental law of radioactivity decay.

$$\frac{dN}{dt} = -\lambda N \tag{1.1}$$

Where N is the number of radioactive nuclei and λ is defined as the decay constant.

The unit of activity has been curie (ci) as exactly 3.7×10^{10}disintegration/second. Which owes its definition to its origin as the best available estimate of the activity of 1 gram pure ^{226}Ra.

Although still widely used in the literature, the curie is destined to be replaced gradually by its SI equivalent, the becquerel (bq). The becquerel defined as one disintegration per second, has become standard unit of activity. Thus

$$1bq = 2.703 \times 10^{-11} ci$$

1.3 Alpha decay

Heavy nuclei are energetically unstable against the spontaneous emission of an alpha particle(or He^4 nucleus). The probability of decay is governed quantum mechanically by the barrier penetration mechanism. The half -life of useful sources varies from days to

many thousands of years. The decay process is written schematically as

$$X_Z^A \rightarrow Y_{Z-2}^{A-4} + \alpha_2^4$$

Where X and Y are the initial and final nuclear species.

The alpha particle appear from a given radioactive source in one or more energy groups that are ,for all practical purposes of monoenergitic. For each distinct transition between initial and final energy level of nucleus(e.g between ground state and ground state), a fixed energy difference or Q-value characterizes the decay. This energy is shared between the alpha particle and the recoil nucleus in a unique way, so that each alpha particle appears with the same energy given by Q(A-4)/A. There are many practical instance in which only one such transition is involved and for which the alpha particles are therefore emitted with a unique single energy may involve more than one transition energy so that the alpha particles appears in groups with differing relatives intensities.

It is no accident that most alpha particle energies are limited to between 4 and 6 Mev. There is a very strong correlation between alpha particle energy and half-life of the parent isotope, and those with the highest energies are those with the shortest half-life.

Beyond about 6.5Mev, the half -life can be expected to be less than a few days, and therefore the source is very limited utility. On the other hand,if the energy drops below 4Mev, the barriers penetration probability become very small and the half-life of the isotope is very large.

Because alpha particle lose energy rapidly in material, alpha particle source that are to be nearly mono-energetic must be prepared in very thin layers. In order to contain the radioactive material, typical sources are covered with a metallic foil or other material that must be also be kept very thin if the original energy and mono-energetic nature of the alpha emission are to be preserved. **?**

1.4 Beta decay

The most common source of fast electrons in radiation measurement is a radioisotope that decays by bet-minus emission. The process is written schematically

$$Z^x \rightarrow Y_{Z+1}^A + \beta^- + \nu$$

Where X and Y are the initial and final nuclear species and ν is the antineutrino. Because neutrinos and antineutrinos have an extremely small interaction probability with matter. They are undetectable for all practical purposes. The recoil, which is ordinarily below the ionization, and therefore it can not be detected. By conventional means. Thus, the only significant ionizing radiation produced by beta decay is the fast electrons or beta particle itself.

Because most radionuclides produced by neutron bombardment of stable material are beta-active, a large assortment of beta emitters are readily available through production in a reactor flux. Species with many different half-lifies can be obtained. Most beta decays populate an excited state of the product nucleus, so that the subsequent de-excitation gamma rays are emitted together with beta particles in many common beta sources.

Each specific beta decay transition is characterized by a fixed decay energy or Q-value. Because the energy of the recoil nucleus is virtually zero. This energy is shared between the beta particle and the "invisible" neutrino. The beta particle thus appears continues.

With an energy that varies from decay to decay and can range from zero to the "beta endpoint energy", which is numerically equal to the Q-value. The Q-value for a given decay is normally quoted assuming that the transition takes place between the ground states of both the parent and daughter nuclei. If the transition involves an excited state of either the parent or the daughter, the endpoint energy of corresponding beta spectrum will be changed by the difference in excitation energies. **?**

1.5 Gamma decay

Gamma radiation is the spontaneous emission of γ-quanta by the nucleus.By emitting γ -quanta, the nucleus goes over from an excited state to a state with a lower energy (radiative transition). There are single radiative transition when the nucleus emits a single quantum and at once goes over to the ground state. Or cascade transitions when the excitation is removed by a successive emission of several γ -quanta.

The energy E_γ of a γ-quantum is determined by the difference in the nuclear energy

levels E between which the radiative transition occurs. According to the laws of conservation of energy and momentum, we have

$$E = E_\gamma + T_{nuc} \qquad\qquad 0 = P_\gamma + P_{nuc} \tag{1.2}$$

Where T_{nuc} and P_{nuc} are the kinetic energy and momentum of the recoil nucleus respectively. From these, we can easily obtain an estimate for T_{nuc}.

$$T_{nuc} = \frac{E_\gamma^2}{2M_{nuc}C^2} \simeq \frac{E^2}{2M_{nuc}C^2} \tag{1.3}$$

This gives $T_{nuc} \simeq 0.1ev = (10^{-6} - 10^{-5})$E for $E \simeq 0.1 - 1Mev$ and for nuclei with $A \simeq 10^2$. Thus, the $\gamma-$quantum carries away an overwhelming part of the nuclear excitation energy. From the above discussion it is obvious that the $\gamma-$quantum spectrum is discrete.

There are different reasons for which a nucleus may turn out to be in an excited state. For example, an alpha or beta decay can leave the nucleus in an excited state. An alpha decay is usually followed by the emission of low-energy $\gamma-$ quanta ($E_\gamma < 0.5Mev$), since an alpha decay followed by the creation of a highly excited daughter nucleus ($W > 0.5Mev$) is hindered because of a low barrier penetrability for low energy $\alpha-$particles. The energy of $\gamma-$ quanta emitted by a daughter nucleus after the beta decay may be higher and attains values up to 2-2.5Mev. This is due to the fact that the probability of beta decay is determined by a weaker energy function than the alpha decay probability.

In both example considered above, the nucleus emitting $\gamma-$ quanta has a comparatively low excitation energy which is not sufficient for the emission of a nucleon. This result can be extended to many other processes leading to the creation of nuclei with an excitation energy lower than the separation energy of a nucleon. These processes include various nuclear reactions involving a nucleus in an excited state as a product. In these cases the excitation energy of the daughter product is smaller than the separation energy of a nucleon(or some other particle), and the emission of $\gamma-$ quanta is the only possible way of removing the excitation (if we do not take into account the processes of internal conversion and the formation of $(e^+ - e^-$pairs).

If the excitation energy of the daughter nucleus is equal to (or higher than) the nucleon separation energy, the emission of $\gamma-$quanta may dominate when the emission of nucleons is hindered due to some reasons. We shall consider the radiative capture of

slow neutrons, when the nuclear excitation due to the capture of a neutron is removed by the emission of two or three $\gamma-$quanta. The emission of $\gamma-$quanta in this case is more probable than the separation of the neutron, since the latter requires the concentration of the entire excitation energy at one nucleon which has to be near the nuclear boundary. This phenomenon is improbable since the binding energy carried by the neutron is distributed immediately after capture among all the nucleons in the nucleus. **?**

The emission of $\gamma-$ quanta by nuclei excited to energies much higher than the separation energy for a particle is associated with the forbiddenness in parity and angular momentum for the escape of nucleons(or other particles), making the emission of $\gamma-$ quanta relatively more probable. An example of this type is the emission of $\gamma-$quanta with energy $17Mev$ as a result of the reaction **?**

$$Li_3^7 + P \rightarrow Be_4^8 + \gamma$$

The $\gamma-$quanta emitted by the nucleus during a transition to a lower energy state may carry away different angular momenta l. The radiation carrying angular momentum $l = 1$ is called the dipole radiation, for $l = 2$ it is called the quadrapole radiation, for $l = 3$ the octapole radiation, and so on. Each of these radiation is characterized by a definite angular distribution. Gamma-quanta of different multipolarities are the result of different types of "oscillation" of the nuclear fluid. Viz. electric (E_1 dipole radiation, E_2 quadrapole radiation, and so on) and magnetic (M_1 dipole radiation, M_2 quadrapole radiation, and so on) in the liquid drop model of atomic nucleus.

The first type of processes are caused by a redistribution of the electric charges in the nucleus, which the second type of processes are due to a redistribution of the spin and orbital magnetic moments. The redistribution of neutrons for which Z+0 must also lead to the emission of electric $\gamma-$quanta, since the motion of the a neutron is accompanied by the emergence of charged recoil nuclei.

A more clear idea about the mechanism of gamma transition can be formed on the basis of a specific model of the nucleus. Thus,in the single -particle model, the emission of the $\gamma-$ multipole is associated with the transition of a nucleon between two single-particle levels differing in their angular momenta by $\Delta I = l$. **?**

1.5.1 Gamma transition probability and selection Rules

In view of the small magnitude of the electromagnetic interaction constant $a = \frac{e^2}{\hbar c} = 1/137 \ll 1$, the probability P of radiation transition can be calculated by the time-dependence perturbation theory method.

$$P = \frac{2\Pi}{\hbar} \mid M \mid^2 \frac{dn}{dE} \tag{1.4}$$

Here, $M = \int \Psi_f^* H^| \Psi_i d\varsigma$ is the matrix element of the Hamiltonian of interaction between the electromagnetic field on the one hand, and charges and magnetic moments on the other hand; $\Psi_f and \Psi_i$ are the wave-function of the final and initial state of the nucleus respectively; dn/dE is the density of the final states .

Electromagnetic theory can be used to write the expression for $H^|$ and dn/dE. Hence the probability P can be estimated by using some model of the nucleus (for example, the shell model) to obtain $\Psi_f and \Psi_i$. The following very rough conclusion can be drawn from the result of the theory.

The radiation field of the moving charges can be represented as a series of spherical function. If the dependence on the coordinates and angles is neglected, we are left with the factor R/λ in the first term of the series(corresponding to the dipole radiator and the quantum with moment $l = 1$), where R is the nuclear radius and λ is the wavelength of the emitted radiation. The second term $(l = 2)$ corresponds to$(R/\lambda)^2$, and the l^{th} term to $(R/\lambda)^l$. Thus for normal values of $E_\gamma = 1Mev$ for nuclei in the middle of the periodic table (A=10^2), we have

$$\frac{R}{\lambda} = \frac{RE}{2\Pi\hbar c} = \frac{6 \times 10^{-13} \times 1.6 \times 10^{-6}}{2\Pi \times 10^{-27} \times 3 \times 10^{10}} \simeq 10^{-3} - 10^{-2}$$

i.e the series converges rapidly. Since P is proportional to $|M|^2$, we obtain for $\gamma-$ quanta with multipolarity l.

$$P_l \propto (R/\lambda)^{2l} \propto A^{2l/3} E^{2l} \tag{1.5}$$

Thus, as l increases by unity, the radiation intensity decreases by a factor of about $p_{l+1}/p_l \propto (R/\lambda)^2 \simeq 10^5$. This means that the first nonzero term in the series (which may not correspond to $l = 1$ due to the selection rules) is the decisive one.

The same conclusion can be drawn regarding magnetic multipoles. For same values of l, however, the intensity of magnetic radiation is $(d/\mu)^2$ times lower than that of the electric field, where d and μ are the electric and magnetic moments of the nucleus.

This is due to different structures of the hamiltonian $H^{|}$ contains the nuclear magnetic moments. For A$\simeq 10^2$. The quantity$(d/\mu)^2$ is approximately equal to

$$(\frac{eR}{e\hbar/m_Nc})^2 = (\frac{m_NcR}{\hbar})^2 \approx 10^2 - 10^3.$$

The set of possible values of l_E and l_M is determined by the angular momentum and parity selection rules. According to the first selection rule, there must exist the following relation between the angular momentum l carried away by the $\gamma-$ quantum, and the angular momenta I_i and I_f of the initial and final states of the nucleus.

$$|I_i - I_f| \leq l \leq I_i + I_f \tag{1.6}$$

According to the second selection rule, the angular momenta l_E and l_M of the electric and magnetic gamma radiation must be connected with the parities P_i and P_f of the initial and final states through the relations.

$$\frac{P_i}{P_f} = (-1)^{l_E} \qquad\qquad \frac{P_i}{P_f} = (-1)^{l_M+1} \tag{1.7}$$

It follows from these relation, for example, that the E_l-transition is possible only between nuclear states with different parties, while the parities of the nuclear states must be the same for the M_l transition. In both the cases, the nuclear angular momenta must satisfy the relation $\Delta I = 0, \pm 1$ (with the exception of the (0-0) transition)

The parity selection rules can be obviously obtained by considering the structure of the matrix element.

$$M = \int \Psi_f^* H^{|} \Psi_i d\varsigma \tag{1.8}$$

In the case of the E_1 -transition,$H^{|}$ in this matrix element contains the electric dipole moment which is transformed as a polar vector upon coordinate inversion. For the M_1-transition, $H^{|}$ contains the magnetic dipole moment having the properties of an axial vector. Taking into account all the above-mentioned features of the gamma radiation, viz

1) A decrease in the the gamma transition probability with increasing l.

2) A relatively small probability of magnetic transition in comparison with electric transition for the same value of l.

3) Angular momentum and parity selection rules.

we arrive at the following conclusion.

The dominating role in the radiative transition between two nuclear states with given P_i, P_f and ΔI is played by electric or magnetic multipoles with the lowest values of l_E and l_M satisfying the angular momentum and parity selection rules:

$$l = |\Delta I| \qquad and \qquad l = |\Delta I| + 1 \tag{1.9}$$

One of these multipoles must be electric,and the other magnetic. Table 1 describes the main gamma transition for some values of $|\Delta I|$ when the parities of the initial and final states are the same or different.

Table 1.1: Describes the main gamma transitions for some values of $\mid \Delta I \mid$ when the parities of the intial and final states are the same or different

$\frac{p_i}{p_f}$		$\|\Delta I\|$		
	0	1	2	3
-1	$\underline{E_1}, M_1$	$\underline{E_1}, M_2$	$\underline{M_2}, E_3$	$\underline{E_3}, M_4$
+1	$\underline{M_1,}, E_2$	$\underline{M_1}, \underline{E_2}$	$\underline{E_2}, M_3$	$\underline{M_3}, E_4$

Naturally the following transition must be excluded from the list of possible transition: (0-0) transition for $|\Delta I| = 0$; (0-1) and (1-0) transition (at l=2) for $|\Delta I| = 1$; (0-2) and (2-0) transition (at l=3) for $|\Delta I| = 2$ and so on.

AS a rule, one of the two main gamma transition considerably predominates over the other due to a strong dependence of the gamma radiation probability on l (the dominant transition is underlined in the table)

In order to obtain a rough estimate of the absolute values of half-live $T_{1/2}$ for different gamma transition, we can use the Weisskopf formula obtained on the basis of the single-particle model of the nucleus under the assumption that the gamma transition is caused by the transition of one nucleon from one single-particle states in to another.

$$W_{El} \propto E^{2l+1} A^{2l/3} \qquad W_{Ml} \propto E^{2l+1} A^{(l-1)2/3} \tag{1.10}$$

Besides the spin and parity selection rules, gamma transition must satisfy the selection rules for isospin. For gamma radiation of many multipolarity, these rules have the

following form: Change in isospin(ΔT) between the state be;

$$\Delta T = 0 \pm 1 \qquad\qquad and \Delta T = 0$$

The experimental data available do not contradict these rules. For some nuclei, it was shown that the gamma transition from a level with $T = 2$ to a level with T=0 occurs not directly, but in a cascade-like manner through an intermediate level with T=1.

Gamma radiation is studied experimentally in the secondary processes accompanying the propagation of $\gamma-$ quanta trough matter, viz.photoelectric effect, *compton effect*, and formation of electron -positron pairs. All these processes involve electrons the magnitude and direction of electrons momenta can be used to form an idea about the energy and direction of the $\gamma-$ quanta inducing them.

The method of investigation of electrons appearing in the photoelectric effect is a lot more accurate. Here the energy of the electrons is uniquely determined by the energy of the $\gamma-$ quanta (and the electron binding energy in the atom). In this method, thin foil of heavy materials (like lead) serve as the source of photoelectrons.

Scintillation counter are used quite successfully in gamma spectrometry in view of their high efficiency. Besides, semiconductor detectors (made of silicon and germanium) are used because of their high resolving power. The gamma spectrometry based on the Mossbuur effect has an absolutely unique resolving power. **?**

1.5.2 Internal Conversion of Gamma ray

Besides the emission of $\gamma-$ quanta, their is another mechanism for the loss of excitation energy, viz. The emission of internal conversion electrons. It is shown by the theory that the nucleus excitation energy in this process is directly (without an intermediate emission of a $\gamma-$quantum)transferred to an orbital electron (overlapping of nuclear and electron wave-function). In this mechanism, obviously, mono-energetic electrons will be emitted, whose energy is determined by the energy of nuclear transition and the type of electron shell. The process of internal conversion has the highest probability for the k-electrons. In this case

$$T_e = E - I_K \tag{1.11}$$

Where T_e is the kinetic energy of electrons and I_k is the ionization potential for the k-electrons.

However, if the energy E released during a nuclear transition is less than the binding energy of the k-electrons, the k-conversion becomes impossible from the energy point of view and L-conversion is observed. From the vary nature of the phenomenon it follows that the conversion radiation must always be accompanied by the emission of characteristic X-rays and Auger electrons.

A typical beta spectrum with sharp peaks corresponding to the emission of conversion electrons. The peaks of conversion origin are usually marked on the beta spectrum by the symbol e^-. The same symbol is used in the energy level diagrams to mark transition accompanied by the emission of internal conversion electrons.

The conversion radiation may be observed with the gamma radiation or without it (in the case of (0-0) transition). The ratio of the number of emitted conversion electrons to the number of emitted $\gamma-$ quanta is called the internal conversion coefficient:

$$\alpha = \frac{N_{e^-}}{N_\gamma} = \alpha_k + \alpha_L + \alpha_M ..... \tag{1.12}$$

Here $\alpha_K = \frac{(N_e)_k}{N_\gamma}$ is the partial internal conversion coefficient for shell electrons, α_L is the corresponding coefficient for l-electrons, and so on.

The investigation of internal conversion is very important for determining various characteristic of nuclear levels (energy levels from the energy of conversion electrons, angular momentum from the conversion coefficient and so on).

Besides the processes of emission of $\gamma-$ quanta and the internal conversion, the transition of an excited nucleus to the lowest state can also occur through the emission of an electron-positron pair. (if the transition energy ($\Delta E > 1.02 Mev$):however the probability of such a transition does not exceed a thousandth part of the gamma radiation probability. **?**

Chapter 2

Absorption of gamma ray

The absorption of gamma radiation through different material is of wide interest for industrial, medical and agricultural studies. It is necessary in the treatment of shielding problem, testing of material, oil-well logging, quantitative measurement of tracers where the active substance can not separated, as in biological or medical measurement in vivo, and finally for the determination of gamma ray energies, either to identify a radioisotope or to established a decay scheme. Absorption gamma rays experiment consists of two parts: measurement of the absorption coefficient of lead for gamma radiation of ^{60}Co under correct condition: measurement in standard arrangement mostly encountered in tracer work. **?**

2.1 Interaction of gamma rays with matter

Because of their electromagnetic nature, gamma rays interact principally with the shall electrons and the coulomb field of the nuclei. Three main process can be distinguished: *photo effect*, *compton scattering*, and *pair production* **?**

2.1.1 Photo effect

The gamma quantum is absorbed by an atomic electron, which is then ejected from the atom. The gamma ray energy is converted into kinetic energy of the photoelectrons and

ionization energy of the atom (binding energy of the electron in its shell). **?**

$$h\nu = E_{kin} + E_B \tag{2.1}$$

The photoelectrons have, therefore, discrete energies $E_{kin} = h\nu - E_k, h\nu - E_l, h\nu - E_m$ according to whether they are ejected from the k, l,or m shell. Although the energy is conserved in the process, the momentum can be conserved only with aid of the recoiling nucleus (the recoil energy is neglected in the above equation) as a consequence the probability of photo effect is largest for the electron coupled most strongly to nucleus, the K electrons, and it increases with this coupling i.e with Z. The exact dependence of the atomic cross section σ_{ph} on nuclear charge and gamma ray energy is quit complicated. In the X- ray region ($< 100kev$) one finds experimentally

$$\sigma_{ph} \cong consZ^4E^{-4} \tag{2.2}$$

At higher energies the exponent of Z is closer to 5: the exponent of E to 3.5. For $E_\gamma >> m_oc^2$, the decreases of σ_{ph} with energy is again slower.

$$\sigma_{ph} \cong consZ^5E^{-1} \tag{2.3}$$

2.1.2 compton effect

If low-frequency electromagnetic wave (light) are scattered by the electrons of an atom, the final state of the atoms is, in the simplest case, identical with the initial states. The scattered light has the same energy (frequency)as the incident wave, the recoil energy of the whole atom being negligible. As the energy of the quanta is increased beyond the binding energies of the electrons, the probability for this coherent scattering decreases. The scattering process becomes independent of the state of electrons: and it can be treated as a collision with a free electrons, in this case, momentum and energy must be conserved between the incident photo, the scattered quantum and the recoil electrons, obviously the energy $h\nu$ of the scattered photon will be smaller than that of the primary gamma ray because of the transfer of energy to the electron. The result of the elementary calculation is

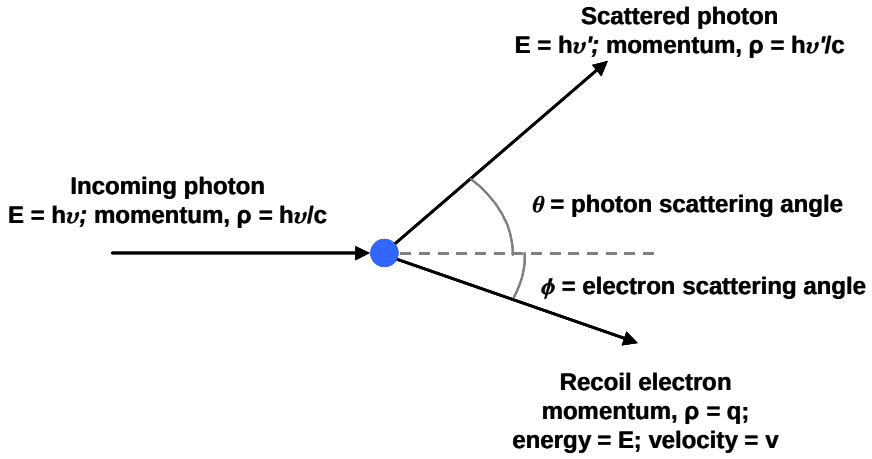

Figure 2.1: compton scattering

$$h\nu^{'} = \frac{h\nu}{1 + h\nu/m_o c^2(1 - \cos\Theta)} \tag{2.4}$$

Where $m_o c^2$ is the rest energy of the electron, $511kev$, and the angle through which the photon is scattered. From the above equation one can write in terms of increases in wave length.

$$\Delta\lambda = \lambda^l - \lambda = \frac{h}{m_o c^2(1 - \cos\Theta)} \tag{2.5}$$

$\frac{h}{m_o c^2} = \lambda_o = 2.43 \times 10^{-10} cm$ are being called the *Compton wave length* of the electron. The energy of the recoil electron is given by

$$E_{kin} = h\nu - h\nu^l = \frac{h\nu}{1 + \frac{m_o c^2}{h\nu(1-\cos\Theta)}} \tag{2.6}$$

$$\cos\Theta = 1 - \frac{2}{(1+\alpha)^2 \tan^2\Phi + 1} \tag{2.7}$$

It will be maximum if the gamma ray is scattered backward.

$$E_{max} = \frac{h\nu}{1 + \frac{m_o c^2}{2h\nu}} \tag{2.8}$$

The cross section of an electrons for *Compton effect* has been calculated by Klein and Neshine. For low energies it has the classical value given by Thomson

$$\sigma_o = \frac{8\Pi}{3} r_o^2 = \frac{8\Pi}{3} (\frac{e^2}{m_o c^2})^2 \tag{2.9}$$

Where $\frac{e^2}{m_o c^2}$ is the classical electron radius $r_o = 2.82 \times 10^{-13} cm$. The cross-section decreases with increasing energy, first as

$$\sigma_e \sim \sigma_o (1 - 2\frac{h\nu}{m_o c^2} .....) \tag{2.10}$$

And for higher energies somewhat more slowly than $\frac{1}{h\nu}$ the atomic cross section is $\sigma_c = Z\sigma_e$. **?**

2.1.3 Pair production

In this process, the gamma quantum disappears and an electron -positron pair is created. The energy of balance require that

$$h\nu = 2m_o c^2 + E^- + E^+ \tag{2.11}$$

Momentum conservation, however, can be obtained only if the process occurs in the neighborhood of a nucleus which recoils. As in the case of photo effect, the atomic cross section depends strongly on the nuclear charge. It is proportional to Z^2. it increases rapidly near the threshold, approximately according to $(h\nu - 2m_o c^2)^2$ but only slowly at higher energies.

The ultimate fate of the positron is annihilation. After they are slowed down by ionization loss in the same way as electrons, they eventually combine with an atomic electron. Their rest energy is dissipated in the form of two gamma quanta each of energy $h\nu = m_o c^2$, travelling in opposite direction. As required by the law of conservation of momentum. **?** The formation of electron-positron pair is explained by Dirac's hole theory. The cross section for pair production varies as; **?**

$$\sigma_p = Z^2 * (h\nu)^b \tag{2.12}$$

These are not the only processes that gamma rays interact with matter. The other processes by which gamma rays interact with matter. The contribution of these processes to μ in the energy range of our interest is certainly low, but we shall mention them for the sake of completeness, these are:

- *Rayleigh scattering*: the process is the coherent scattering of gamma rays from bound atomic electrons, Rayleigh scattering is predominant at low photon energies, small scattering angle and high Z absorbers.
- *Thomson scattering* : this process includes coherent scattering of gamma rays by (a) free electrons and (b) nucleus as a whole(nuclear Thomson scattering)
- *Nuclear photodisintegration* : in this class of processes gamma rays are absorbed by the nuclei and nucleons are ejected from the nuclei. Such processes $(\gamma, p), (\gamma, n)$ etc. Occur only at high gamma ray energies.
- *Nuclear resonance scattering* : these process involve the energy levels of the nuclei. Which are excited by resonant absorption of gamma rays. The resonant excitation of the levels is followed by emission of gamma rays during de-excitation.
- *Delbruck scattering:* in this process photons are scattered by the coulomb potential of the nucleus. **?**

2.2 Absorption coefficient of gamma rays

Consider a beam of x-rays or gamma rays, such that I is the intensity of photons falling perpendicularly on a slab of material of thickness Δx. Then the number of photon ΔI, removed from the beam due to the interaction of gamma rays with matter is proportional to the thickness and the number of incident photons N. **?** Thus

$$\Delta I = -\mu I \Delta x \tag{2.13}$$

Where μ is the proportionality constant is known as the total linear attenuation coefficient. The intensity of gamma rays thus decreases with the absorber thickness. The attenuation coefficient μ depends on the material and on the energy of the gamma rays

. For a given material and monochromatic gamma rays μ will be constant and we can integrate equation 2.11, to obtain

$$I = I_o e^{-\mu x} \tag{2.14}$$

Where $\mu = n(\sigma_{ph} + \sigma_c + \sigma_p)cm^{-1}, and\ I_o$is the intensity of the incident beam, while I is the intensity of the beam after traversing a distance x in the absorber. n is the number of atoms per cm^3. Thus, the intensity of gamma ray beam of particular energy passing through homogeneous material follows an exponential law of absorption, in contrast to a definite rang which characterizes charged particles. The linear absorption coefficient μ has units cm^{-1}.

For the typical energies of gamma rays encountered in nuclear spectroscopy (say from 0.1Mev to 10.0Mev) there are three important processes by which photons interact with matter and lose their energy. These are:

- Photoelectric effect, predominate in the energy rang 100Kev to 500kev.
- Compton effect, important in the energy rang 100kev to 1.0 Mev
- Pair production, possible only when energy is above 1.02Mev.

The linear attenuation coefficient μ is built from contribution from all these above processes because they are independent of each other. Thus equation 2.13 can be extended to write

$$Photoelectric\ effect \qquad (\Delta I)_{ph} = -\mu_{ph} I \Delta x \tag{2.15}$$

$$Compton\ effect \qquad (\Delta I)_c = -\mu_c I \Delta x \tag{2.16}$$

$$Pairproduction \qquad (\Delta I)_p = -\mu_p I \Delta x \tag{2.17}$$

adding up the three equation

$$(\Delta I)_{total} = (\Delta I)_{ph} + (\Delta I)_c + (\Delta I)_p \tag{2.18}$$

$$(\Delta I)_{total} = -(\mu_{ph} + \mu_c + \mu_p) I \Delta x \tag{2.19}$$

$$(\Delta I)_{total} = -\mu I \Delta x \tag{2.20}$$

Where μ_{ph}, μ_c, and μ_p are the partial attenuation coefficients arising out of photoelectric

effect, Compton effect and pair production respectively, from equation 2.18 we have, **?**

$$\mu = \mu_{ph} + \mu_c + \mu_p \tag{2.21}$$

It is often useful to measure the surface density (d)of the absorber instead of its thickness X. If ρ is mass density $d = \rho x$, and more usually a total mass attenuation coefficient μ_m is used. It is defined by $\mu_m = \mu/\rho$. Then equation 2.11 becomes.

$$I = I_o e^{-(\mu/\rho)d} \tag{2.22}$$

The mass absorption coefficient is normally expressed in cm^2/g or (cm^2/mg) (μ and μ/ρ are often used indiscriminately similarly, d and X may both be called "thickness" of the absorber.

The absorption law holds for the number of gamma quanta of the original energy present in the beam after traversing a thickness x of absorber. In performing an absorption experiment, care must be exercised to avoid the measurement of scattered quanta which would tend to decrease the apparent value of the absorption coefficient. Three types of scattered radiation must be prevented from reaching the counter.

- *radiation is easily scattered from the surroundings*. This is minimized by suspending source and counter at a large distance from solid matter. The only background scattering then is due to the air and is therefore very small.

- A *gamma ray which, with out absorber, does not hit the counter is scattered in to the counter by the absorber*. This is prevented by reducing the size of the absorber so that it intercepts only the direct beam (shaded part). In order for this to be possible, the absorber must be at a certain distance from the source.

- *A photon may be scattered through a small angle only, so that it still reaches the counter.* This error is diminished by reducing the solid angle subtended by the counter at the absorber. Considering (b), and (c), the absorber is placed about midway between source and counter **?**

If the source is a positron emitter, additional precautions are necessary because of the annihilation radiation. It is produced wherever the positrons come to rest. Spurious variations of the gamma intensity can arise if absorbers are brought near an unprotected

β^+ source, e.g the gamma intensity of an uncovered β^+ emitter rises if an absorber is placed behind it: the best practice is always to enclose a positron emitter in an absorber thick enough to stop all positrons.

Since the scatter-free suspension is not practical for general laboratory use, it is replaced in the experiment by the other extreme of collimating the gamma ray beam through a channel cut in lead.

For weak activities the distance between sample and counter must be small. In this case no collimation is possible. The absorption can be measured in a shelf type of stand in the same way as the beta absorption. The apparent absorption coefficient will be decreased by the scattered radiation and increases by oblique passage of the gamma rays through the absorber. The net effect depends on the geometry used , and the correction must be found by measuring the absorption coefficient of gamma rays of known energies such as the radiation of ^{60}Co and the annihilation radiation. **?**

Chapter 3

Radiation detectors

3.1 Introduction

In the present chapter we shall discuss the three types of gamma ray spectrometer. The field of gamma ray spectroscopy is one of the most highly developed techniques in experimental nuclear physics because gamma ray detection and gamma spectrum determination forms the essential measurment at every step in nuclear spectroscopic experiments. Until recently sodium iodide scintillation spectrometer was the most successful and popular method of gamma ray spectroscopy. The scintillation spectrometers with their high detection efficiency and moderatly good energy resolution have made a tremendous contribution to our present knowledge of nuclear properties. The recent development of semiconductor radiation detectors (particularly of the Ge(Li) detectors) has further revolutionized our experimental techniques and has helped us to push the frontier of our knowledge to newer horizons. **?**

3.2 Scintillation detector

A large number of the fundamental experiment in nuclear physics have been performed by microscopic examination of the scintillation of the phosphor ZnS under the impact of alpha particle with the development of electronic techniques, the scintillating screen was replaced by pulse ionization chambers and Geiger counter. Only when the G-M counter

proved inadequate for the high activities obtainable with modern machines, and unreliable for the measurement of time interval appreciably short than $1\mu s$, was the scintillation method resumed. The subjective observation has been replaced by the registration of the light flash with the aid of multiplier phototube followed by an amplifiers and recorder. **?**

There are several substances, certain organic and inorganic materials, which emit light flashes or scintillation when charged particles ray or gamma -ray pass through them. These substances are called *scintillator*. In a scintillation detector these light flashes are allowed to fall on the photo cathode of a photo multiplier tube and a pulse is extracted out to Signal the passage of nuclear radiation. The height of this output pulse can be made proportional to the energy dissipated by the ionizing radiation in the scintillator. Thus a scintillation detector can be used not only for counting but for energy analysis also. Because of its versatility, there has been considerable development of scintillation detectors. We describe the operations of a scintillation detector a step-by-step. **?**

3.2.1 Operation of scintillation detector

The other thing is the operation of scintillation detector. The main operation of scintillation detector is as follows. We shall describe the operation of a scintillation detector step by step.

1. *The absorption process*: a charged particle falling on a scintillation can dissipate all its energy in its if the dimensions of the scintillator are large compared to its range. If a gamma ray (x-ray) is incident on a scintillator it may interact with matter in three way, *photoelectric effect*, *Compton effect*, And *pair production*. In each of this effect, electrons are produced and by successive interactions the gamma rays can transfer all or part of its energy in to the kinetic energy of such secondary electrons. These secondary electrons will give up their kinetic energy in ionization or excitation in the scintillation material.

2. *The scintillation process*: the scintillator absorbs energy when it undergoes ionization and excitation by the electrons. This absorbed energy appears either as heat energy (in more than 60 percent cases) or as luminescence photons. In the latter process, the excited states of the scintillator material de-excite to lower states by

light emission within 10^{-8} seconds or less. This emitted light is known as scintillation. The time dependence of the photon emission follows an exponential law.

$$N_p = cons(1 - e^{-t/\tau}) \tag{3.1}$$

Where N_p is number of light photons emitted in the time t after the ionization radiation has arrived, and τ is decay time or time required for the emission of 63% of the photons. Each scintillation materials has a characteristic mean life t.

3. *Conversion of light into electrical pulse*: the light emitted by the scintillator is allowed to fall on the photocathode of a photomultiplier tube, which is optically coupled to the scintillator. The scintillation is enclosed in an envelope having reflecting walls and the scintillator is transparent to its own radiation. As a result depending on the geometry and the optical properties of the system certain fraction of light produced in the scintillator falls on the photo cathode of the photomultiplier tube producing photoelectrons. The structure of a photomultiplier tube is such that there are several dynodes as shown in fig 3.1. And these are maintained at successively higher electrical potential (about 100 volt per dynode stage) further the dynode surfaces have a property of emitting more(say 3-5) secondary electrons when one incident electron strikes them. Thus a photoelectron emitted by a photocathode is accelerated by the electric field to the first dynode where it produces a bunch of secondary electrons. These electrons are now accelerated towards the next dynode. Where they intern, produce more electrons and this process is repeated at each dynode.

In a photomultiplier tube there are usually 10 or more dynodes stages and one can usually achieve a gain up to 100 by the time electrons reach the last stage which is called the anode. In this way the initial ionizing radiation gives rise to a burst of electrons at the anode where an electrical pulse is taken out from further analysis.

Many photomultiplier tubes have been developed commercially and today one has a choice of several versatile photomultiplier tubes. The photocathode in these tubes is usually a semitransparent coating of some photoemission material. (e.g antimony-cesium) on the inner surface of the flat top of the tube envelope. The spectral sensitivity of such photocathodes usually follows a response curve. The quality of a photomultiplier

tube is mostly determined by two properties (i) the transit time or the time taken by the electrons to reach the anode through the dynode structure. This property is important for the timing characteristic of the photomultiplier tube (ii) the stability of the electron multiplication factor. This property determines the energy resolution characteristics of the photomultiplier tube.

We now prove that the amplitude of the pulse appearing at the out put of a photomultiplier tube is proportional to the energy of the incident nuclear radiation. The pulse height V at the output will be related to the amount of charge collected at the out put through the relation.

$$V = \frac{Q}{C} \tag{3.2}$$

where C and Q are the capacitance in the output point and total charges respectively.

If the incident nuclear radiation has energy $E_n(ev)$, a fraction f_n of this energy will be dissipated in the scintillator. If this energy $f_n E_n$ is converted into light energy by the scintillator with an efficiency E_l then an amount $E_l f_n E_n$ is the amount of light energy produced in the scintillator. If f_p is the fraction of photon which reach photocathode then an amount $f_p E_l f_n E_n$ of light energy reaches the photocathode when an $1.0ev$ of light strikes it and let f_d be the fraction of photoelectrons collected by the dynode. If the electron multiplication factor is M_1, then the total number of electron reaching the final stage will be

$$N_e = M f_d f_m f_p E_l f_n E_n \tag{3.3}$$

$$Q = N_e e = e M f_d f_m f_p E_l f_n E_n \tag{3.4}$$

Thus finally

$$V \alpha E_n \tag{3.5}$$

We thus see that final pulse height in a scintillation detector is proportional to the initial energy of the incident particle. **?**

3.2.2 Scintillation gamma rays spectrometer

One of the most efficient method of counting gamma rays and measuring their energies is their detection by a scintillation gamma ray spectrometer. This spectrometer employs a scintillation detector which is usually a thallium activated sodium iodide [NaI (Tl)]

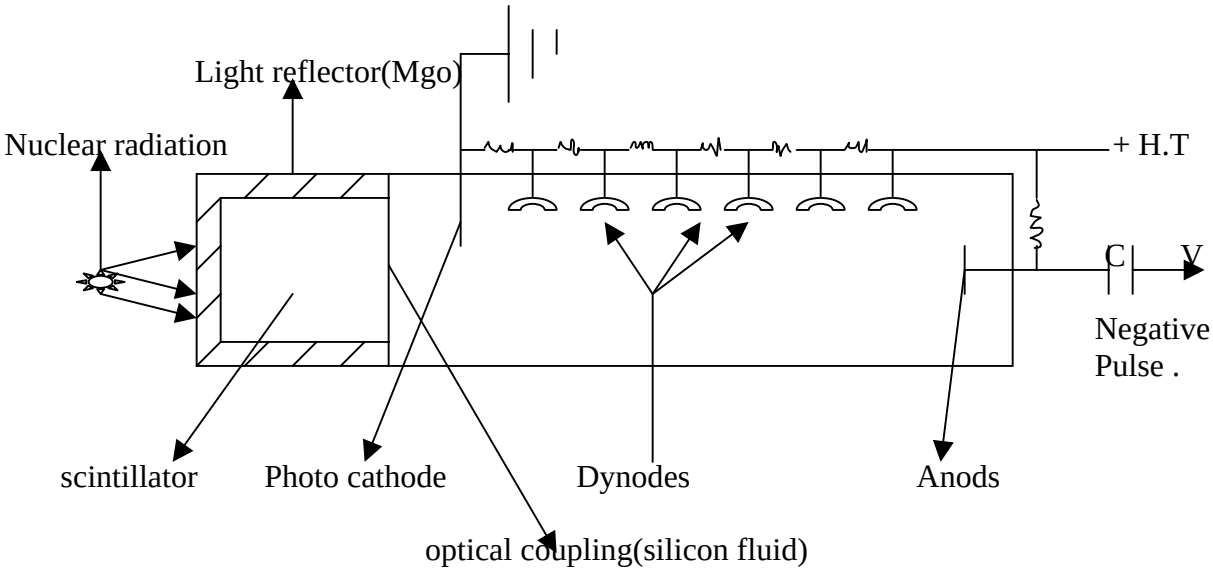

Figure 3.1: schematic construction of a scintillation detector

crystal as a scintillatior. The NaI (Tl) crystal, being hygroscopic, is hermetically sealed in an aluminium can a shown in fig 3.2. Further, the scintillator is covered on all sides by a layer of reflecting material like MgO or Al_2O_3 powder. A glass window is provided at one end so that light produced by the scintillator can pass on to the photocathode. The NaI (Tl) crystals are usually in the form of right circular cylinders, their dimension being determined by the needs of the particular measurement.

Let us understand the interaction of an incident gamma ray with the scintillation detector. we shall assume that the scintillation detector is coupled to the nuclear electronic system. as in figure 3.2.

If a mono-energetic gamma ray of energy E_o were to be detected by such a scintillation spectrometer, a theoretical plot of N the counting rate per unit energy (pulse height) interval versus energy (pulse height) E should appears as line spectrum as in fig 3.3. However,owing to various affects, the observed spectrum is never so simple. To understand the complex nature of the actually observed spectrum, a discussion of various absorption processes is necessary.

a) *Photoelectric absorption* :- For some gamma rays the iodine X-ray may escape the crystal without being absorbed. In this case, we shall observe another peak, the

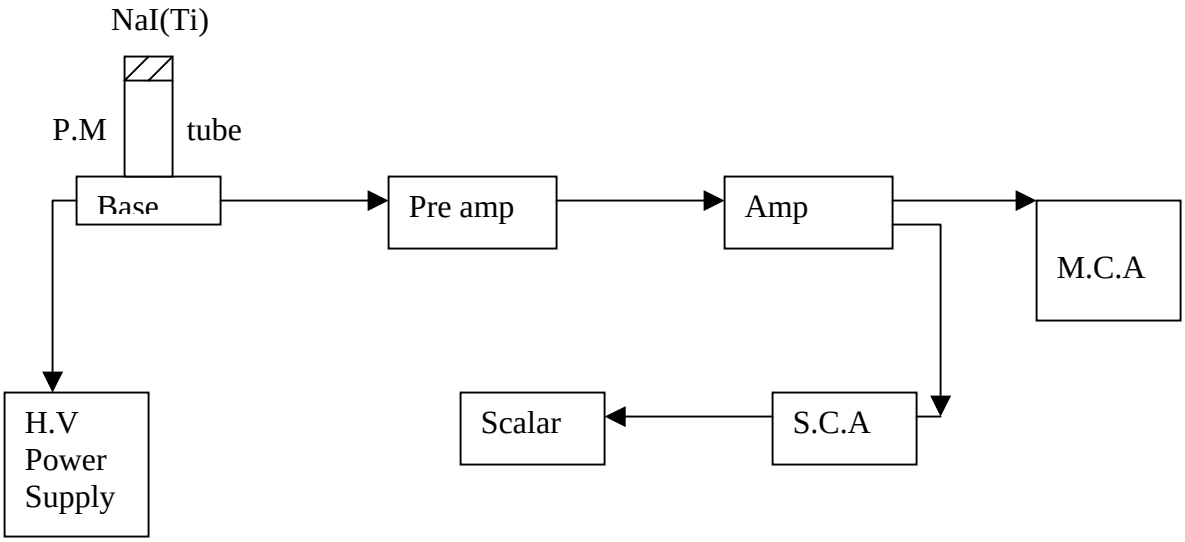

Figure 3.2: Nuclear electronic system of a scintillation spectrometer

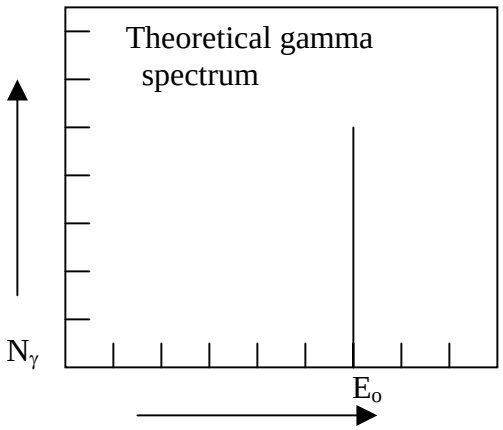

Figure 3.3: Theoretical gamma spectrum (plot of gamma ray counting rate verses gamma ray energy)for monoenergtic gamma ray

escape peak, at a lower energy equal to (Eo - 20)Kev corresponding to this partial absorption of the gamma ray. Because of the finite resolution of the spectrometer the escape peak looks resolved from the photo -peak only for $Eo < 100Kev$. An example of the escape peak is shown in fig 3.5. The flow diagram of gamma rays undergoing photoelectric absorption in a scintillator. A gamma ray of energy E_o undergoing a photoelectric effect within the NaI (Tl) crystal will eject an electron from the atomic shells. The emitted photoelectron will have a kinetic energy $K = (E_o - 28Kev)$, where 28kev is the binding energy of the electron in an iodine atom. Immediately after the photoelectric absorption of gamma ray, the binding energy of the electron appears in the form of X-ray and or auger electrons.

Almost all of the these X-ray are immediately absorbed in the surrounding material of the scintillator, their energy being given up to photoelectrons created. In this way, the entire energy E_o of the incident gamma ray is absorbed and is finally converted into light photons, theoretically the energy spectrum corresponding to this total photoelectric absorption will give rise to a line spectrum or a single (full energy) photo peak as in fig 3.4.

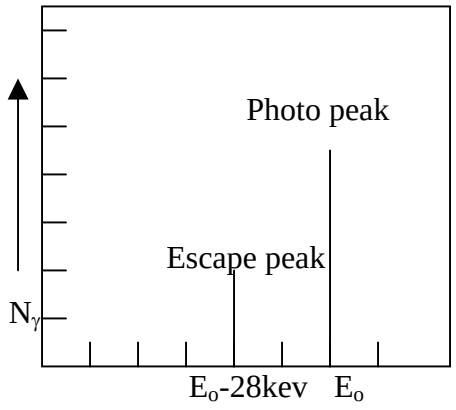

Figure 3.4: Theoretical gamma spectrum arising out of photoelectric interaction of monoenergitic gamma ray

For some gamma rays the iodine X-ray may escape the crystal without being absorbed. In this case, we shall observe another peak, the escape peak, at a lower

energy equal to $(E_o - 20)Kev$ corresponding to this partial absorption of the gamma ray. Because of the finite resolution of the spectrometer the escape peak looks resolved from the photo -peak only for $E_o < 100Kev$. An example of the escape peak is shown in fig 3.4.

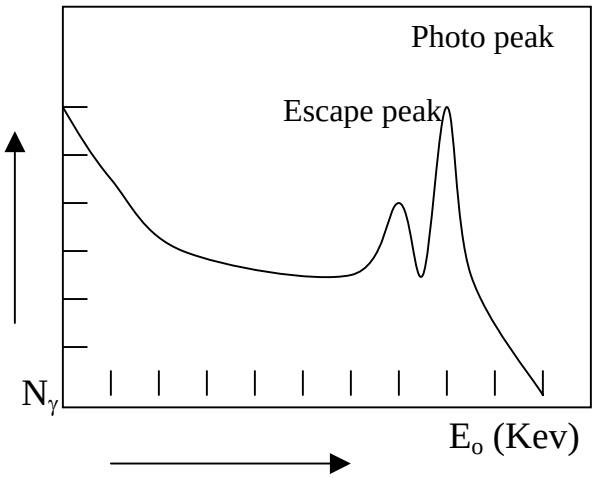

Figure 3.5: Gamma spectrum (hypothetical)showing photo peak accompanied by escape peak

It is observed that even the photo peak corresponding to the total absorption of the gamma ray energy E_o does not appear as a line spectrum.

The widening of line into a gaussian -shaped profile figure 3.8 is the effect of finite resolution of the system. This broadening is due to the statistical fluctuations in the various processes with convert the gamma rays into an output pulse. Thus each of the processes, i) conversion of incident gamma rays into luminescence photons, ii) light transmission and collection by the photo cathode, iii) focusing of the photo-electrons on the dynodes and v) multiplication of the electrons in the dynode stages, contribute to the statistical fluctuations and subsequent broadening of the line.

b) *Compton effect absorption* : - when the incident gamma ray undergoes Compton scattering in the scintillator it gives part of its energy to the recoil electron. The Compton electron will have an energy,

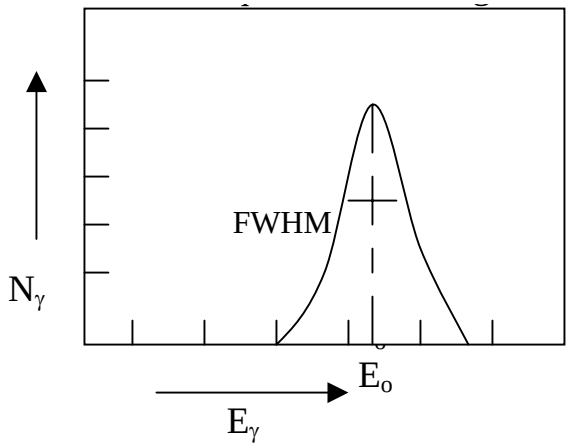

Figure 3.6: Effect of finite resolution of the photo peak

$$E_o = E_o - \frac{E_o}{1 + \alpha(1 - \cos\Theta)} \tag{3.6}$$

$$E_e = E_o[\frac{\alpha(1 - \cos\Theta)}{1 + \alpha(1 - \cos\Theta)}] \tag{3.7}$$

Where α is defined as $\frac{E_o}{m_o c^2}$.

depending on the scattering angle Θ, the compton electron will, therefore, have a continuous energy distribution ranging from a minimum zero $(\Theta = 0)$ up to a maximum.

$$E_e = \frac{2\alpha E_o}{1 + 2\alpha} \tag{3.8}$$

Obtained by putting $\Theta = \Pi$ in equation above. This maximum limit of the energy spectrum of the Compton electron is usually called the Compton edge.

Thus the incident gamma rays of energy E_o will give rise to Compton electrons of energies between 0 and E_o in the scintillator and the corresponding scattered gamma rays may be completely stopped in the scintillator through photoelectric effect or successive Compton effect or they may escape the scintillator without detection. In the former case the gamma rays energy spectrum will show a full energy peak figure 3.7 at Eo. In case the Compton scattered gamma ray are not stopped in the crystal. It will give rise to a continuous spectrum fig 3.7 from 0 to E_e, because the Compton

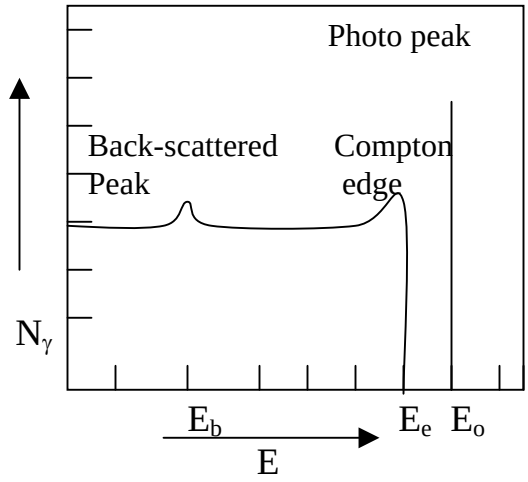

B)

Figure 3.7: Theoretical gamma spectrum arising out of the compton interaction of monoenergtic gamma ray.

electrons are stopped in the crystal. The spectrum becomes peaked near the Compton edge. There is another phenomenon contributing a small peak at lower energies. There is always some materials surrounding the scintillator and some gamma rays can undergo compton scattering in this material with $\theta = \Pi$. Such backscattered gamma rise to a peak at energy E_b. The value of E_b can be calculated $(\Theta = \Pi)$ from above equation.

$$E_b = \frac{E_o}{1 + 2\alpha} \tag{3.9}$$

And it is usually in the region 150 -300 Kev for $E_o < 1Mev$.

C) *Absorption by pair production:-* the incident gamma ray will interact with the crystal through pair production only if its energy is greater than $1.02Mev$. In this process the gamma ray energy E_o is given up in creating the pair of an electron and positron, the energy of the pair being $E_p = (E_o - 1.02)Mev$. The electron is stopped in the crystal while the positron is annihilated: and the annihilation is accompanied by two oppositely directed gamma rays of total energy $1.02Mev$. Both or one of the

annihilation gamma rays (each having through processes (a) and (b) above) or they can escape the crystal. In case both the photons are completely stopped in the crystal one will get a full energy peak at E_o. If one or both gamma rays escape we should get a corresponding peak at energies E_o - $m_O c^2$ or $E_o - 2m_O c^2$ as shown in figure 3.8.

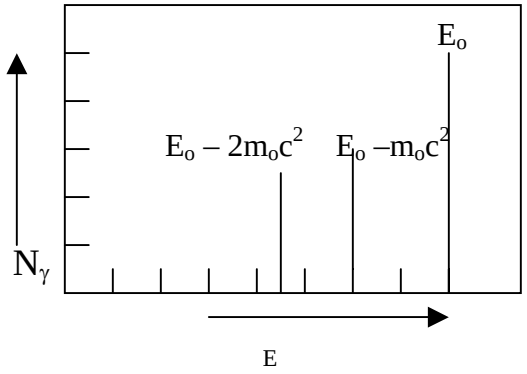

Figure 3.8: Theoretical gamma spectrum arising out of the pair production interaction of a monoenergtic gamma ray.

We have now seen how an incident gamma ray, through various interactions with the scintillator, can give rise to various parts of the gamma ray spectrum. The relative cross section for various processes depend on the energy of the gamma ray as shown in the above discussion .

Above discussion indicates that occurrence of various processes also depend upon the scintillator size and source scintillator geometry. Larger volume of the scintillator, greater is its efficiency to absorb the gamma rays completely

An actually observed gamma ray spectrum will be a supper imposition of the spectra figure 3.4, 3.7A and 3.8, of course modified by the spectrometer resolution.

The detection efficiency η of a scintillator crystal must be known if any quantitative measurement are desired. The efficiency η is determined by the following factors.

I) the energy of gamma rays.

II) the type of scintillator crystal used.

III) the type of geometry used. This includes the size of the crystal, the dimension of the source, the relative position of source and the crystal. **?**

3.3 Semiconductor radiation detector

The development of semiconductor radiation detectors during the last decade has completely revolutionized the field of nuclear radiation detector. As an analogy, they can be considered as ionization chambers where the gaseous medium is replaced by a semiconducting solid. In a semiconductor detector ionizing radiation produces ion pairs which are collected by the electric field applied externally, and the detector gives an electric pulse which is proportional to the energy of ionizing radiation. The semiconductor detector have many definite advantages over the gas filled or scintillation detector. some of these advantages are.

i) Smaller, compact and convenient size,

ii) Fast (few n sec) rise time of output pulses.

iii) Linear response over wide energy range.

iv) Excellent energy resolution.

v) Choice of sensitive depth, area and geometry

In the initial stages of development the detector were designed for detection of heavy charged particles. Very soon development of semiconductor detector for electrons and gamma rays followed.

Today complete system of the semiconductor radiation detectors and associated electrons is available entirely commercially and extensive use of these detectors is being made in nuclear spectroscopy. **?**

3.3.1 Lithium-drifted germanium detector

Lithium -drifted germanium [Ge(Li)] detectors are more suitable than silicon detectors for the detection of electromagnetic radiation. It may be recalled that the photoelectric absorption cross section for gamma rays is proportional to Z^5 and therefore germanium (Z= 32) is more efficient than silicon (Z= 14) for detection of gamma rays.

A Ge(Li) detector consists of an (n-I-p) junction device prepared by a careful process outlined below. The first step is usually the preparation of a cylindrical piece of high quality p-type germanium by zone refining techniques. The next step is to diffuse lithium ions into the germanium so that a n-type region is formed. The lithium ions are then allowed to drift towards the central core under the action of intense electric field. The whole process is carefully controlled. The drifted ions of lithium are effective in compensating or neutralizing the p-type impurities in germanium and they give rise to a region of intrinsic or high resistivity material.

The intrinsic region forms the active volume of the detector where ionizing radiation (gamma rays) create hole-electron pairs which are collected by external electric field. The Ge(Li) detector is always maintained in low temperature.enviroment to keep up the intrinsic character of germanium. In practice, the low temperature environment is maintained by a cryostat and liquid nitrogen $(77^{o}k)$ dewar which together with the Ge(Li) detector form a compleat detector system. Today compleat Ge (Li) detector system offering large sizes ($> 20cm^{3}$) and high energy resolution are commercially available. It may be added that the nuclear electronics associated with the semiconductor radiation detectors has to be more sophisticated as compared to other detectors. **?**

3.3.2 Ge (Li) gamma ray spectrometer

The development of lithium drifted germanium [Ge(Li)] detectors during the last decade has ushered a new era in gamma ray spectroscopy.

The energy resolution of Ge(Li) spectrometers is 10-20 times better than that of NaI(Tl) detectors. Recently, large Ge(Li) detector $(> 30cm^{3})$ have become commercially available and their photo peak efficiencies are almost comparable to that of medium sized NaI(Tl) detectors. Today Ge(Li) detectors are extensively used to detect X-rays and gamma rays up to $\sim 20Mev$ energies.

The basic detection mechanism of a Ge(Li) detector has already been discussed in the above. A lithium drifted intrinsic region is sandwiched between a n-type layer and a p-type layer of germanium the incident gamma rays interact with the atoms of the detector material through photoelectric effect, compton effect or pair production. Secondary electrons produced in these processes give rise to electron-hole pairs which are collected by the electric field applied across the crystal.

One handicap of the Ge(Li) detector is that it has to be operated at $77^{o}k$ (or liquid nitrogen temperatures) in order to keep the leakage current at a lowest acceptable value. The detector is usually kept in vacuum maintained by the Zeolite sorption pump or an ion pump. The detector characteristics worsen if it is exposed to room temperature for a longer period .

The energy resolution obtainable with a Ge(Li) gamma ray spectrometer is limited by the following factors.

I) The statistical fluctuation in the number of ion pairs created for a given energy E is an important factor which limits the resolution.

II) The electronic noise contributed by the preamplifier and amplifier of the spectrometer system is another important factor.

III) Other factor which affect the energy resolution are stability of the whole system,charge collection efficiency of the system etc.

In view of the excellent resolution of the Ge(Li) detector, the energy determination of the Ge(Li) gamma ray spectrometer has to be made very carefully.

The peak position is carefully determined by knowing the peak profile. Often this analysis is performed with a computer programme. In addition, the statistical of the data will also affect the accuracy involved.

The linearity of the system is measured with an electronic pulses. various gamma rays standards are used to check the response of the detector and to calibrate the spectrometers. Energy standards available over a wide range of gamma rays energies are listed by marion[6] and are also given.once the energies of some gamma rays of a given spectrum are reliably determined,one can use these for internal calibration.

The efficiency of the Ge(Li) detector must be determined before any quantitative analysis of the relative intensities of the gamma rays is possible. **?**

3.3.3 Germanium gamma -ray detector(HPGe)

I) General consideration

The simple junction and surface barrier detectors find widespread application for detection of alpha particles and other short-range radiations but are not easily

adaptable for application that involve more penetrating radiations. Their major limitation is the maximum depletion depth or active volume that can be created. Using silicon or germanium of normal semiconductor purity, depletion depth beyond 2 or 3 cm are difficult to achieve despite applying bias voltages that are near the breakdown level. Much greater thickness are required for the detectors intended for gamma-ray spectroscopy, which are the topic of this note. The thickness of the depletion region is given by

$$d = (\frac{2\epsilon v}{eN})^{1/2} \tag{3.10}$$

Where v is the reverse bias voltage and N is the net impurity concentration in the bulk semiconductor material (ϵ is the dielectric constant and e is the electric charge) at a given applied voltage, greater depletion depth can be only be achieved by lowering the value of N through farther reduction in the net impurity concentration. **?**

II) Configuration of Germanium Detector

A) High-purity Germanium (HPGe) detector fabrication.

Techniques for the production of ultrapure germanium with impurity level as low as 10^{10} atoms/cm^3 first were developed in the mid 1970s. The starting material is bulk germanium intended for use in the semiconductor industry. This material, already of high purity, is further processed using techniques of zone refining. The impurity levels are progressively reduced by locally heating the material and slowly passing a melted zone from one end of the sample to the other. Since impurities tend to be more soluble in the molten germanium than in the solid, impurities are preferentially transferred to the molten zone and are swept from the sample. After many repetitions of this process, impurity levels as low as 10^9 atoms/cm^3 have been achieved. The resulting germanium is perhaps the most highly purified and completely analyzed material of any kind that has ever been produced in commercial volume. Large single crystals of germanium are then slowly grown from this purified feed stock. If the remanning low-level impurities are acceptors (such as aluminum) the electrical properties of the semiconductor. Crystal grown from the material is mildly

p type (The designation Π type is often used to represent this high-purity p-type material). Alternatively, if donor impurities remain, high purity n type (designated $\nu - type$) is the result.

B) Planar Configuration.

A representative configuration for a planar HPGe detector fabricated from high-purity p-type (or $\Pi - type$ germanium is shown fig 3.9. In a planar configuration, the electrical contacts are provided on the two flat surfaces of a germanium disk. The n^+ contact can be formed either by lithium evaporation and diffusion on to one surface of the wafer, or by direct implantation of donor atoms using an accelerator. The detector depletion region is formed by reverse biasing this n^+ p junction. The contact at the opposite face of the crystal must be a noninjecting contact for a majority carrier. It may consist of a p^+ contact produced by ion implantation of acceptor atoms, or a metal-semiconductor surface barrier that acts as the electrical equivalent. Ion implantation technique have the advantage that the contact layer can be made very thin to serve as entrance windows for weakly penetrating radiations such as low -energy X-ray.

High-purity germanium detectors are generally operated as fully depleted detectors. Reverse biasing requires that a positive voltage be applied to the n^+ contact with respect to the p^+ surface. The depletion region effectively begins at the n^+ edge of the central region and extends deeper into the Π region as the voltage is raised until the detector becomes fully depleted. Further increases in the voltage then serve to increase the electric field every where in the detector by a uniform amount.

Germanium detectors may also be fabricated starting with high-purity n-type material (also known as $\nu - type$) rather than with p-type material as described above. And therefore the configuration choice has a more significant influence on the details of the charge carrier motion.

C) Coaxial Configuration.

For the planar detectors outlined above, the diameter of the cylindrical crystal from which the wafer is cut is typically no more than a few centimeters. The maximum depletion depth (or thickness of the lithium-drifted region) is limited to less than 1 or 2 cm. The total active volume available in planer detectors

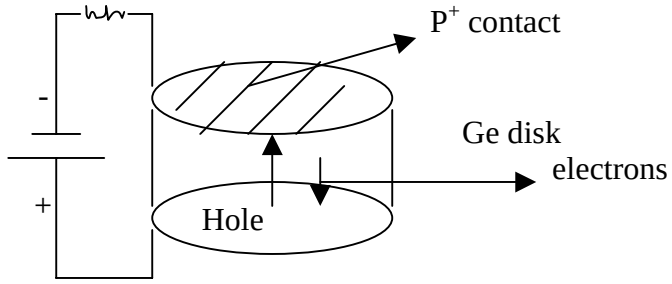

Figure 3.9: Configuration of a planer HPGe detector.the Ge semiconductor may be ν type (p^+ contact is rectifying),Π type (n^+ contact is rectifying),or lithium drifted

therefor does not exceed about 10-30 cm^3. To produce a detector with a larger active volume as needed in gamma -ray spectroscopy, a different approach is used. The detector is then constructed in cylindrical or coaxial geometry as illustrated in fig 3.10. In this case, one electrode is fabricated at the outer cylindrical surface of a long germanium cylindrical crystal. A second cylindrical contact is provided by removing the core of the crystal and placing a contact over the inner cylindrical surface. Because the crystal can be made long in axial direction, much larger active volumes can be produced (up to 750cm^3 at the time of this writing). An added advantage of coaxial geometry is that, by using a small inner diameter, larger-volume detector can be fabricated with lower capacitance than would be possible using planar geometry.

A closed-ended coaxial configuration is one in which only part of the central core is removed and the outer electrode is extended over one flat end of the cylindrical crystal (see fig 3.10).

In coaxial geometry, the rectifying contact that forms the semiconductor junction can in principle be placed either at the inner or outer surface of the crystal. The electric field conditions that result are quite different.

III) Germanium detector operational characteristics

A) Detector cryostat and dewar.

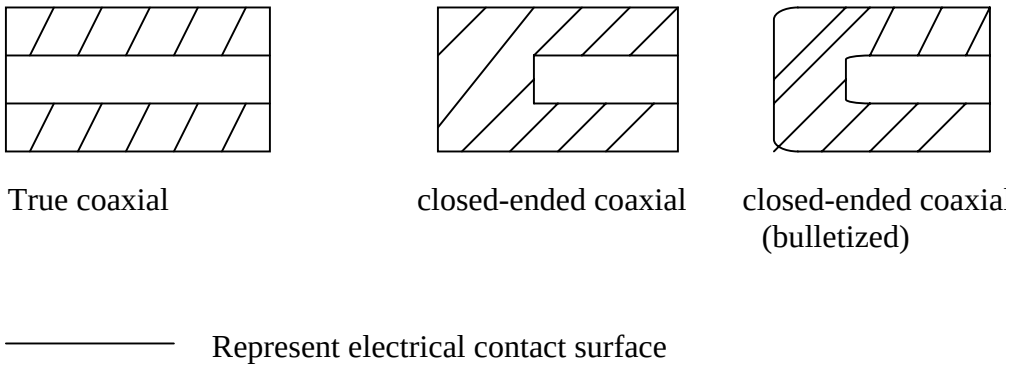

Figure 3.10: The three common shapes of large-volume coaxial detectors.Each represents a cross-section view through the axis of a cylindrical crystal

Because of the small band gap (0.7ev), room-temperature operation of germanium detectors of any type is impossible because of the larger thermally-induced leakage current that would result. Instead, germanium detectors must be cooled to reduce the leakage current to the point that the associated noise does not spoil their excellent energy resolution. Normally, the temperature is reduced to 77^ok through the use of an insulated dewar in which a reservoir of liquid nitrogen is kept in thermal contact with the detector.

Although it is conventional to operate HPGe detectors at liquid nitrogen temperature, in some applications it may be more convenient to allow the detector temperature to rise above this nominal 77^ok value. Several studies have shown that the performance of coaxial detectors does not suffer until the absolute temperature rises to about $130k$. **?**

B) Energy Resolution The dominant characteristic of germanium detectors is their excellent energy resolution when applied to gamma -ray spectroscopy. The greater superiority of the germanium system in energy resolution allows the separation of many closely spaced gamma -ray energies, which remain unresolved in NaI(Tl) spectrum. Consequently, virtually all gamma-ray spectroscopy that involves complex energy spectra is now carried out with germanium detectors. **?**

3.4 Multichannel analyzer

3.4.1 The analog-to-digital converter

The general specifications are: the job to be performed by the ADC is to derive a digital number that is proportional to amplitude of the pulse presented at its input. Its performance can be characterized by several parameters.

I) The speed with which the conversion is carried out.

II) The linearity of the conversion, or the faithfulness to which the digital output is proportional to the input amplitude.

III) The resolution of the conversion, or the "fineness" of the digital scale corresponding to the maximum range of amplitude that can be converted.

3.4.2 The Memory

The memory section of an MCA provides one addressable location for every channel. Any of the standard types of digital memory can be used, but there is sometimes a preference for "nonvolatile" memory,which does not require the continual application of electrical power to maintain its contents. Then, data acquired over long measurement periods will not be lost if the power to the MCA is accidentally interrupted.

3.4.3 Dead time

. The dead time of an MCA is usually comprised of two components the processing time of the ADC and the memory storage time. For a Wilkinson-type ADC, is a variable time that is proportional to the channel number in which the pulse is stored. The processing time per channel is simply the period of the clock oscillator. For atypical clock frequency of $100MHz$ this time is 10ns per channel once the pulse has been digitized, an additional fixed time of a few microseconds is generally required to store the pulse in the proper location in the memory. Thus, the dead time of an MCA using an ADC of this type can be written.

$$\tau = \frac{N}{\nu} + B \tag{3.11}$$

Where ν is the frequency of the clock oscillator, N is the channel number in which the pulse is stored, and B is the pulse storage time.(**?**)

3.5 Single-Channel Analyzer

Another linear-to-logic converter is widespread use involve two independent discrimination levels. A differential discriminator or single -channel analyzer (SCA) produces a logic output pulse only if the input linear pulse amplitude lies between the two levels. The action of the unit is therefore to select a band of amplitude or window in which the input amplitude must fall in order to produce an output pulse.

Several systems of nomenclature and adjustment persist for SCAs. In some units, the lower-level discriminator (LLD) and upper-level discriminator(ULD) are independently adjustable from front-panel controls. In others, the lower level is labelled the E level, and the window width or difference between levels is labelled ΔE and can be varied separately without affecting the E level.

In counting the systems, the SCA can serve to select only a limited range of amplitudes from all those generated by the detector. In normal SCAs, the time of appearance of the logic pulse is not closely coupled to the actual event timing, and use of these logic pulse in timing measurements will often give imprecise results. If one of the time pick-off methods is incorporated into the SCA design, the logic pulse can be much more closely correlated with the actual event time. Modules with this feature are often called SCAs and widely used in coincidence applications or other time measurement.

Most SCAs provide the option of switching out the upper-level discriminator and using the unit as a simple integral discriminator controlled by the lower level. The input linear pulse are intended to be shaped with typical 0.0s-10 μs widths and a pulse height range that most commonly is 0-10V positive. Bipolare pulse with positive leading edges are also normally acceptable. Other specification that can be important is some applications include the linearity of the discriminator level adjustments. The stability of the levels with respect to temperature changes, and the SCA dead time.

Chapter 4

Instruments

4.1 Gamma ray source

A number of radiation source are available mounted in small plastic rods and are kept in a lead container. ^{137}Cs,^{60}Co,and ^{57}Co are used as a gamma rays source. The source are not strong. The radiation level is (1-0.1μCi) by standard. These sources were stored in a lead contained during experiments not to interfere the counting.

4.2 Gamma ray detector

4.2.1 The coaxial germanium detector

The coaxial germanium detector is basically a cylinder of germanium with n-type contact on outer surface, and a p-type contact on the surface of an axial well. The germanium has a net impurity level of around $10^{10} atom/cm^3$. Measurement have been performed using the conventional coaxial HPGe detector with a 12.5% relative efficiency and a resolution of $1.9 kev$(FWHM at $1.33 Mev$). The useful energy of the detector is above $40 kev$ to more than $2 Mev$. An experimental quantification of spectra by 4096 channel and channel width $\Delta E = 1.9V$ has been utilized.

4.2.2 Scintillation detector of NaI(Tl)

The gamma ray detector is a scintillation detector consisting of a scintillation crystal, a photomultiplier tube,and a preamplifier assembled in a single unit. The crystal is a 3

inch diameter, 3inch thick NaI crystal doped with Thallium. The photomultiplier is a maximum voltage rating of 100 volts and with 10 dynodes. The photomultiplier anode output is connected to an amplifier by a short length of coaxial cable.

4.3 Amplifier

The amplifier accepts both positive or negative input pulses and provides both pulse shaping and amplitude expansion of these pulses. The amplifier gain is set via a central knob setting and there are both unipolar positive going outputs on connectors. The function of the amplifier is to produce positive output pulses of suitable amplitude and shape so that they can be feeded into pulse height analyzer.

Shaping time——— $2\mu s$
Coarse gain———- 20V
Fine gain ———7.5V

4.4 Multi-channel pulse height Analyzer

The multichannel analyzer is a Pc contains an ORTEC model 5100 a pulse height analyzer card (MCA) run by the canberra s100 software package. The MCA card contains an analog to digital converter (ADC), single channel analyzer (SCA), Multichannel scaler (MCS), and a dual -ported memory. The card, along with the standard software, transforms the personal computer into a multichannel analyzer. An input of 0 to 10volt positive pulses from a shaping amplifier is the only external signal necessary for pulse height analysis operation. The software is located in MCA directory.

4.5 High Voltage Supply

The high voltage supply for the gamma ray detector is a model 1034A using the positive H.V output connector. The supply can furnish an output of $\pm 0 - 2000V$ Dc. We normally run photomultiplier somewhere between 800-1000volt.

4.6 Micrometer

Micrometer is an instrument used for measuring of the thickness of the absorber. It is divided in 1000 scale because of that it gives us more accurately value of the thickness with an error of 0.01%.

4.7 Lead collimator

The purpose of the collimating holes is to insure that only gamma which are not scattered may reach the detector. Nor a gamma ray has been scattered by the lead or by the absorber then it is unlikely to reach the detector. Because gamma rays are highly absorbed by lead and do not produce radiation.

Chapter 5

Experiment

5.1 Objective of the experiments

1) To measure the total linear attenuation and photo absorption coefficients of six elements in different geometry of absorber.

2) To verify the dependence of attenuation coefficient on the atomic number of the absorber.

3) To verify the dependence of attenuation coefficients on the energy of gamma rays.

4) The effect of the type of the detector used on the measurement of attenuation coefficients.

5.2 Experimental

5.2.1 Set up of the system

The gamma spectrometer Canberra system 100 used in our laboratory consist of a HPGe detector. The resolution and relative efficiency of the detector for 1332kev and ^{137}cs source were 1.82kev and 19.4% respectively. The detector and preamplifier were not placed inside low background lead shield and cooled by liquid nitrogen from vertical distich crostate. The integrated signal processor (model 1510) consist of pulse height analysis system to transform pulses, which were collected and stored by a computer -based MCA. The signal processor contains high-resolutory spectroscopy amplifier with

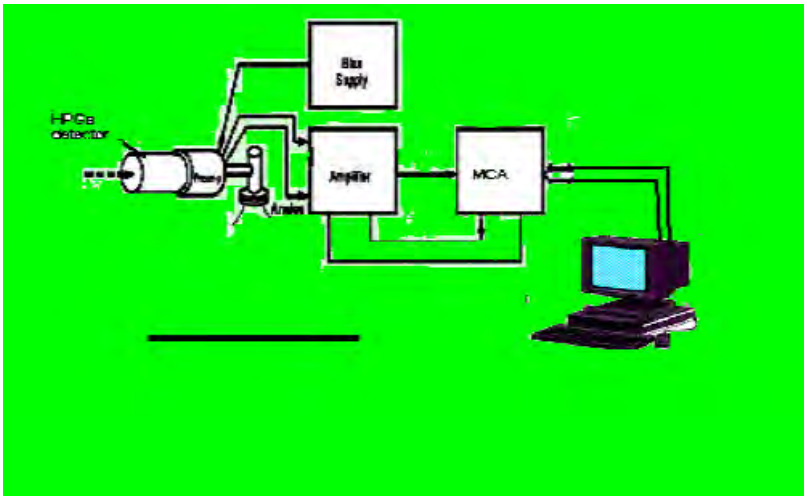

Figure 5.1: Schematic diagram of gamma-rays spectroscopy

a pile-up rejector and live -time corrector, which allows the spectrum analysis nearly independent of a system count rate. In our measurement the input pulse shaping was set to $4\mu s$. The dead time of ADC convertor with a clock rate of 100mHz equals a fixed time of $1.5\mu s$ (for peak detection) plus $0.01\mu s$ multiplied by the channel number. Data were stored in 4096 sequential channels. Automatic correction for the dead time was obtained by collecting data for a given live time. In general, the gross count rates for our samples are low, therefor the random summing correction were neglected.

Operating parameters of the system were governed and controlled by the computer program -canberra system MCA100. The spectrum of laboratory background activity has been established from prolonged measurements. The spectrum analysis was performed in the range up to about $2Mev$. The distance between source and detector was kept fixed at 7cm. In this arrangement there was a provision to increases the absorber thickness up to about 2cm: Lead, copper, tine, nickel, Iron and Aluminium material were used as absorbers. Gamma rays of $662kev$, $1332kev$, $1172kev$, and $122kev$ were obtained from ^{137}Cs,^{60}Co.^{57}Co radioactive isotopes.

5.2.2 Observation of some typical spectra.

The spectrum of pulses from the ^{137}Cs.^{60}Co,^{57}Co and the background were observed and the amplifier gain so that the peak at $662kev$, $1173kev$, $1332kev$, and $122kev$ were located in the upper half of the available range was adjusted.

5.2.3 Measurement of the attenuation coefficient for different elements of using 662Kev gamma ray

The spectrum of the background was taken. And the absorber near to the detector was put, then the photon spectra of ^{137}Cs gamma rays were recorded. By increasing the thickness of the absorbers keeping the collimator size and distance between the source and detector fixed, the spectra of each absorbers for different thickness were taken. An absorber of thickness x, put in the collimated beam will change the beam intensity from I_o to I, following the law, i.e

$$lnI_o - lnI = -\mu x \tag{5.1}$$

The transmitted spectra were recorded for sufficient time for precision and accuracy of the result. The background counts recorded for the same time were subtracted from each spectrum. A $662kev$ peak as" Region of interest"(ROI) and used "sum" counts as a measure of intensity setup. The areas under ROIs were recorded. Using the origin software log of the intensity (area) of gamma ray recorded as a function of thickness of absorber were plotted for each absorbers. Using square fitting method the slope of the graphs were obtained. The slopes of the graph are equal to the attenuation coefficients of the elements. Finally the total linear attenuation coefficient as a function of atomic number Z of the elements was plotted. The whole of the above procedure repeated for the absorber near to the source.

5.2.4 Measurement of attenuation coefficient in Sn as a function of energy of the gamma rays

Gamma rays source of ^{137}Cs, ^{60}Co, and^{57}Co were used. The attenuation in Sn of these gamma rays were measured for absorber near to the detector.

The transmission were measured for different thickness of Sn for each energy. Even if the transmission varies so much with energy, the thickness required for an accurate

measurement will vary with energy. In order to get the various peaks at a reasonable channel position for measurement, the gain of the amplifier was adjusted as the energy of the gamma rays changed. The total linear attenuation coefficients were obtained using the same method like the above, and as a function of energy was plotted.

Finally using NaI(Tl) detector was used to measure the attenuation coefficient of elements for comparison with the HPGe detector. In this case only the detector was changed and the set-up and the method used for HPGe were used again.

5.3 Data Acquisition

The aims of experiments are to show the cross-section of the interaction depend on geometry, atomic number, energy of gamma rays and the type of the detector used. So to get the cross-section the important data needed are the transmitted intensity of gamma rays in different thickness of the six elements. These are shown below.

Table 5.1: Elements used

Elements	Atomic number	Density(gm/cm^3)	number of atoms/cm^3
Pb	82	11.30	0.32826×10^{23}
Sn	50	5.30	0.26911×10^{23}
Cu	29	8.96	0.84918×10^{23}
Ni	28	8.89	0.91202×10^{23}
Fe	26	7.80	0.84118×10^{23}
Al	13	2.70	0.60264×10^{23}

Table 5.2: The total and photo peak intensity of the gamma rays of ^{137}Cs, when absorber near to the detector using HPGe detector

Elements	Thickness (cm)	Total intensity(cd)	Photo peak intensity(cd)
Pb	0.090	17331±3.01%	9769±2.10%
	0.170	16376±3.7%	9145±2.18%
	0.252	15231±2.69%	8471±2.27%
	0.338	14191±3.31%	8005±2.31%
	0.428	13485±1.48%	7397±2.44%
Sn	0.086	17964±2.29%	9975±209%
	0.164	17443±1.80%	9601±2.14%
	0.244	17033±2.53%	9601±2.12%
	0.322	16578±2.38%	9405±2.13%
	0.399	15916±1.84%	8801±2.23%
cu	0.091	13778±1.54%	10570±2.15%
	0.187	12824±1.16%	9717±2.27%
	0.268	12236±1.58%	9303±2.31%
	0.349	11955±1.76%	9167±2.31%
Ni	0.088	18092±2.38%	9967±2.10%
	0.165	17573±2.00%	9794±2.11%
	0.248	16832±1.59%	9375±2.15%
	0.315	16537±1.16%	9084±2.16%
Fe	0.093	17976±2.41%	9975±2.09%
	0.174	17503±1.99%	9712±2.12%
	0.255	17311±1.19%	9440±2.17%
	0.334	16369±1.89%	8982±2.21%
	0.421	15375±1.48%	8692±2.21%
Al	0.091	18359±1.68%	10292±2.05%
	0.171	18240±1.15%	10104±208%
	0.253	17788±2.25%	10018±2.07%
	0.337	17917±2.20%	9953±2.09%
	0.422	16965±1.72%	9882±2.08%

Table 5.3: The total and photo peak intensity of gamma ray of ^{137}Cs, when the absorber near to source using HPGe detector

Elements	Thickness (cm)	Total intensity(cd)	Photo peak intensity(cd)
Pb	0.090	20083±3.12%	14733±1.90%
	0.170	18252±2.78%	13909±1.89%
	0.252	16758±2.51%	12887±1.94%
	0.338	15188±2.11%	11694±2.04%
	0.428	13907±1.54%	10895±2.08%
Sn	0.086	20028±2.35%	15863±1.70%
	0.164	18629±1.24%	14812±1.76%
	0.244	17311±2.33%	13740±1.83%
	0.399	15409±1.96%	12567±1.86%
cu	0.091	21028±1.63%	12520±2.46%
	0.187	20347±1.24%	13532±2.16%
	0.268	19243±1.58%	13501±2.07%
	0.349	18061±1.56%	12975±2.06%
Ni	0.088	20605±2.23%	16299±1.68%
	0.165	19954±2.11%	15999±1.68%
	0.248	18995±1.58%	14960±1.76%
	0.315	18023±1.24%	13898±1.87%
Fe	0.093	20221±2.30%	16375±1.64%
	0.174	18407± 1.99%	14575±1.78%
	0.255	17024± 1.24%	13740±1.80%
	0.334	15679± 1.35%	12685±1.86%
Al	0.091	21193±1.35%	17224±1.59%
	0.171	20465±1.24%	16786±1.60%
	0.253	20160±2.25%	16506±1.61%
	0.337	19112±2.30%	15415±1.70%
	0.422	18556±1.65%	14532±1.80%

Table 5.4: The total and photo peak intensity of gamma ray ^{137}Cs, when absorber is in a better position using NaI(Tl) detector

Elements	Thickness (cm)	Total intensity(cd).	Photo peak intensity(cd).
Pb	0.090	44247±2.11%	38679±2.58%
	0.170	41250±2.00%	35801±2.75%
	0.252	38272±1.52%	31925±3.29%
	0.338	35490±2.41%	29982±3.28%
	0.428	32591±1.42%	28100±3.18%
Sn	0.086	47507±2.35%	41879±2.41%
	0.164	46347±1.42%	41318±2.32%
	0.244	44922±2.36%	38875±2.67%
	0.322	43535±1.34%	36829±2.94%
	0.399	42053±2.41%	35826±2.92%
cu	0.091	47747±1.32%	40981±2.67%
	0.187	46134±1.25%	40626±2.45%
	0.268	44931±1.69%	39602±2.48%
	0.349	42807±1.76%	35383±3.21%
Ni	0.088	47369±2.14%	41382±2.50%
	0.165	45401±2.10%	39414±2.62%
	0.248	42466±1.32%	36658±2.77%
	0.315	44023±1.24%	37796±2.78%
Fe	0.093	48018±2.15%	39276±3.13%
	0.174	46600±1.99%	38218±3.15%
	0.255	45168±1.21%	37564±3.06%
	0.334	43985±1.34%	37339±2.89%
	0.421	42621 ±1.65%	33760±3.64%
Al	0.091	49328±1.65%	43939±2.26%
	0.171	48314±1.32%	41249±2.70%
	0.253	47475±2.32%	41068±2.60%
	0.337	47427±2.01%	40003±2.85%
	0.422	46478±1.65%	39054±2.92%

Table 5.5: Total and photo peak intensity of different energy of gamma ray in Sn using HPGe

Energies(kev)	Thickness(cm)	Total intensity(cd).	Photo peak intensity(cd).
122.00	0.086	2687±3.53%	852±6.37%
	0.164	1661±3.31%	526±8.11%
	0.244	976±3.48%	274±11.45%
	0.322	634±3.21%	148±16.11%
	0.399	413±2.58%	105±18.85%
662.00	0.086	17964±2.29%	9975±2.09%
	0.164	17443±1.80%	9601±2.14%
	0.244	17033±2.55%	9501±2.12%
	0.322	16578±2.38%	9405±2.13%
	0.399	15916± 1.84%	8801±2.23%
1172.00	0.086	10726±1.44%	2337±4.06%
	0.164	10549±1.90%	2465±3.95%
	0.244	10321±1.86%	2385±4.02%
	0.322	10501±1.30%	2303±4.13%
	0.399	10388± 1.06%	2164±4.31%
1332.00	0.086	4468±2.26%	1652±4.85%
	0.164	4338±2.14%	1494±5.19%
	0.244	4409±1.74%	1239±6.00%
	0.322	4259±1.99%	1048±6.77%
	0.399	4154±2.35%	854±7.92%

5.4 Data analysis and Discussion

Using the value of tables 5.2, 5.3, and 5.4 log of intensity versus thickness was drawn as shown in the figure 5.2 only for lead, like that for other elements of attenuation coefficients were obtained. And from the graph by using square fitting method, the slope of the graph was obtained. The slope equal to the attenuation coefficient of material. Their values is given in the tables 5.6, 5.7, 5.10, 5.11.

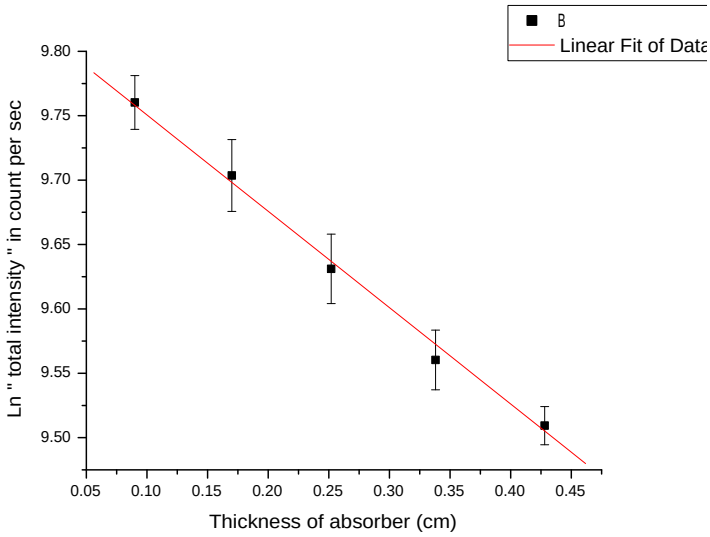

Figure 5.2: Ln of "total intensity" versus thickness of absorbers in lead

Table 5.6: Experimental value of total linear and mass attenuation coefficients using HPGe detector

Element	Near to the detector(cm^{-1})	Near to source(cm^{-1}))
Pb	0.76129±.0311	1.09057±.0199
Sn	0.37344±.0227	0.52846±.0975
Cu	0.55684±.0745	0.59439±.0755
Ni	0.49415±.0318	0.58798±.0792
Fe	0.41344±.0738	0.47569±.0271
Al	0.12495±.0607	0.19702±.0344

Table 5.7: Experimental value of photo absorption coefficient using HPGe detectors

Element	Near to the detector(cm^{-1})	Near to source(cm^{-1})
Pb	0.81840±.0211	0.92390±.0298
Sn	0.34492±.0327	0.47692±.0876
Cu	0.27696±.0654	0.49137±.0523
Ni	0.51240±.0328	0.70932±.0423
Fe	0.42616±.0583	0.46681±.0254
Al	0.13830±.0605	0.14731±.0345

Table 5.8: Experimental value of Linear and mass attenuation coefficient of Sn for different energies using HPGe detector

Energies(kev)	Total (cm^{-1})	Photoelectric (cm^{-1})
122.00	6.00873±.1307	6.96166±.0242
662.00	0.37344±.0227	0.34492±.0117
1172.00	0.28228±.0472	0.08775±.0372
1332.00	0.20877±.05806	0.16762±.0481

The cross-section was calculated using the formula below from tables 5.5, 5.6 the total attenuation coefficient has been taken.

$$\sigma = \frac{\mu}{n} \tag{5.2}$$

Where σ, μ, and n are cross-section, linear attenuation, and number of atoms per unit volume respectively.

Table 5.9: Cross-section of absorber near to the detector using HPGe

Element	Total cross-section in(b)	Photoelectric cross-section in(b)
Pb	23.191578	24.931959
Sn	11.876802	4.990811
Cu	6.557358	6.558535
Ni	5.418192	5.618297
Fe	4.914989	4.265545
Al	2.087129	1.7160975

Table 5.10: Theoretical total cross-section of elements

elements	Total cross-section in barn(b)
pb	25.088931
Sn	10.85704
Cu	5.89038
Ni	5.670547
Fe	5.26461
AL	2.618190

5.4.1 Determination of attenuation coefficient in different geometry of the absorber

From table 5.6 as it is seen, when the absorber near to the detector, the attenuation coefficients of elements are better result as compared to the theoretical value, with an error of 5% to 10%. But for the absorber near to source is with an experimental error of 8% to 13%, this is because of the half acceptance angle. This error is the contribution of many effect, not only the geometry. One of from these is the medium thickness. That mean, with the increases in medium thickness, the probability of multiple scattered photons to be added in the uncollidded beam of 662kev gamma rays increases. The other one is the collimator size. Which also contribute the increases in error, this is because of the probability of counting of more number of single or multiple scattered photons along with the beam of 662kev gamma rays increases due to larger exposure of the detector. So because of the contribution of these effect, the error has been increased. In addition to these the geometry of the absorber also high effect on the value of the attenuation coefficient like collimator size, as it is seen in the table 5.6.

The result of log of transmitted beam verses thickness of absorber for lead are plotted in figure 5.1. From these results, it is seen that at a larger absorber thickness, the transmitted intensity decreases with increasing in absorber thickness at different geometry of the absorber. Further the increases in the transmitted beam is larger for grater half acceptance angle with increases in thickness, which is due to the contribution of counting multiple-scattered photons as has been discussed in the above paragraph. This leads to an increase in the value of attenuation coefficient of the elements. But the counting of multiple scattering effect is reduced when the half acceptance angle is decreased with the absorber near to the detector. Due to this attenuation coefficient is unaffected due to absorber near to the detector. This means that there is definitely some kind of correlation

between the geometry and the attenuation coefficient of the elements. So far as different material are concerned, the effect of sample geometry on the measured attenuation coefficient of the material have been investigated for medium energy gamma rays **?**. In addition to this the type of the detector used also affect the attenuation coefficients. For example in our case HPGe and NaI(Tl) were used. But good result is obtained from HPGe as it is shown in the table 5.6 as compared to table 5.11. This is due to high resolution power of HPGe detector.

Table 5.11: Experimental value of total linear and mass attenuation and photo absorption coefficients using NaI(Tl) scintillator detector.

Element	Total(cm^{-1})	Photoelectric(cm^{-1})
Pb	0.90506±.0068	0.96681±.0052
Sn	0.39084±.0136	0.54522±.0241
Cu	0.41252±.0422	0.53501±.0251
Ni	0.46851±.1894	0.53109±.2540
Fe	0.36298±.0043	0.40234±.0031
Al	0.18874±.0234	0.32091±.0350

5.4.2 Dependence of attenuation coefficient on the atomic number of the absorber.

The result of total cross-section measurements for the six elements are plotted in the figure 5.3. From the results, it is seen that at a larger atomic number, the cross-section increases with increases in absorber atomic number. This is due to the contribution of the increasing binding energy of the electrons. As the atomic number increases in with binding energy increases. This lead to an increase in the value of cross-section. In the theoretical calculation the relation between atomic number and cross-section for total and photoelectric in chapter 2 are given by $\sigma_{ph} \propto Z^5$ and $\sigma_{tot} \propto (Z^5 + Z + Z^2)$,where $\sigma_{ph}, \sigma_{tot}$ and Z are cross-section of photoelectric. Total cross-section and atomic number of the absorber respectively. So the atomic number and the cross-section have direct relation. Our experimental result also shown this effect of atomic number on the cross-section. This lead to change in attenuation coefficient of the elements.

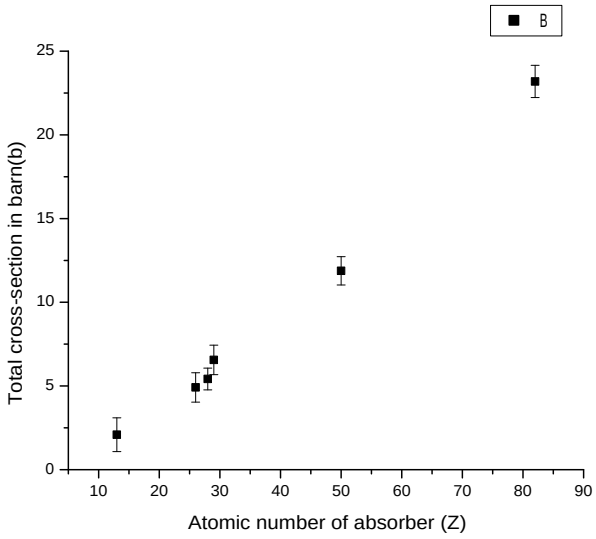

Figure 5.3: Total cross-section versus atomic number of absorbers

5.4.3 Dependence of the cross-section on the energy of the gamma rays.

In this case for different energies of gamma rays, the cross-section were obtained as it is shown in the table 5.12. The result of total linear cross-section measurements are plotted in the figure 5.4. From the graph as it is shown the cross-section decreases as the energies increases. This is due to high penetration power of the gamma ray. That mean, when the energy increased, the probability of interaction of gamma ray with the atomic electron decreases. As a result of this the cross-section decreases. But the energies get larger and larger, the cross-section increases. This is due to the dominate effect of pair production. Which mean in pair production, cross-section is directly proportional to the energies of gamma rays. This leads to the increases in cross-section coefficient. In theoretical calculation also shows at high energies, the cross-section is directly proportional to the energy of gamma rays as it has been discussed in Chapter 2. And our experimental result also shown this effect even if we used small number of energies sources.

The cross-section of tine for different energies is obtained using equation 5.2 and table 5.7 and the value are listed in table 5.12.

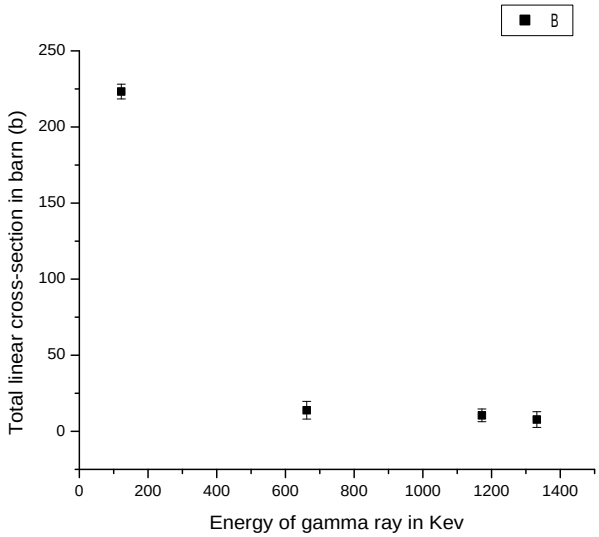

Figure 5.4: Total cross-section versus energies of gamma rays in Sn

Table 5.12: Cross-section of Sn for different energies

Energies(kev)	Total in barn(b)	photoelectric in barn(b)
122.00	223.2807	258.6919
662.00	13.8768	4.9908
1172.00	10.4894	0.3252
1332.00	7.7577	6.2287

5.5 Errors

Sources of random errors include counting statistics, uncertainties in sample thickness, and errors in applying sample impurity correction, shielding problem of a detector.

5.6 Conclusion

From the above discussion, it can be conclude that effect of half acceptance angle in the measurement of attenuation coefficient of the elements can be minimized by using a well geometry of absorber respect to the source and detector. So the effect of large exposure of the detector to the beam decreased by choosing position of the absorber near to the detector. And high resolution power of HPGe detector make HPGe detector good for measurement of attenuation coefficient. Then, it is concluded that with an optimum position of absorber, and using HPGe detector the attenuation coefficient can be measured more accurately for their better use in different practical field.

The Microscopic cross-section interaction of the elements totaly depends on the atomic number and the energies of the source as it is shown in the figures 5.2 and 5.3 respectively. So the one that has large atomic number attenuate the beams more than the one has less. And attenuation of the beam are also decreased when the energies get large as shown in the figure 5.3, Thus the attenuation decreased up to energy of gamma ray is $5Mev$ and increased when the energies get larger.

APPENDIX

Detector specification and performance data of Ge detector.

The coaxial Germanium detector which is used for measurement of photon energy have the following properties.

5.7 specification

Relative efficiency———50%

Resolution ————2.7kev(FWHM) at 1.332Mev

Cryostat description —-U-style integral crystal type 7915.3

5.8 Physical performance data

Geometry———-coaxial one open end, closed and facing window. Diameter——48mm

Length———-34.5mm

Active area facing windows 18.1 cm^2

Distance from windows—5mm

5.9 Electrical characteristic

Depletion voltage——+3000v

Recommended bias voltage —+3500v

leakage current at recommended bias 0.1mA

Abbreviation

MCA——————————— Multichannel analyzer

Mev——————————— Mega electron volt.

Kev——————————— Kilo electron volt

ADC——————————— Analog-to-digital converter.

MCS——————————— Multichannel scaler.

S100—— ——————————- system 100

DC——————————— Direct current

ROI——————————- Region of Interest.

HPGe——————————— Highly Purify Germanium

FWHM——————————— Full Width Half Maximum.

SCA——————————— Single Channel Analyzer.

H.V——————————— High voltage.

P.M——————————— Photo Multiplier.

LLD——————————- Lower Level Discriminator.

ULD——————————— Upper Level Discriminator.

Bibliography

Ernst Bleuler and George J.Goldsmith. *Experimental Nuclenics*. Rineehart and cimpany inc New york, fifth edition, 1952.

S Gopal and Sanjeevaiah. *Nucl.instrum.Methods*, volume 107. 1973.

Parjit S Singa Gurdcep s.sidhu, Karamjit Singh and Gurumels Mudahar. Effect of collimator size and absorber thickness on gamma ray attenuation measurements for bakelite and perspex. *Pramana journal of physics*, 53(5):851–855, November received 26 April 1999;revised 23 july 1999.

Marc lefort Doctor of science;professor at the sorbome. *Nuclear Radiation*. Frist Published in france as les radiation nucleares.and manufactured in the united state of america.

K.N Mulchin. *Experimental Nuclear physics*, volume I physics of atomic nucleus. Moscow, Printed in the union of soviet socialist Republics, 1987.

R.M Singru. *Introduction to Experimental nuclear physics*, wiley eastern private limited new delhi,1972 and revised printing 1974

Glenn F.Knoll John Wiley. *Radiation Detection and measurement*. Third edition. 2000

A.L Conner, H.F. Atwater, and EliZabeth H. Plassmann. *Gamma-ray Attenuation coeffiecient Measurement*. *Physical review A General physic*, -544 University of California, Los Alamos Scientific Labratory,Los Alamas, new mex.co 87544 and J.H. MC Crary. Third series, vol 1,number 3, March 1970.

Charlotte Meaker Davisson and Robley D.Evans. *Gamma ray Absorption Coefficients*. *Review of modern physics*, -107. Massachusetts Institution of Technology,Cambridge. Volume 24, Number 2, April 1995.

Charlotte Meaker Davisson and Robley D.Evans. *Measurements of Gamma -ray Absorption Coefficients. Physical Review*, -411 Massachusets Institute of Technology, Cambrige of Massachuset. volume81, Number 3, February 1, 1951, Receives Decenber 5,1949

DECLARATION

I here under signed declare that the thesis is my original work, has not been presented for a degree in any other university and that all sources of material used for the thesis have been duly acknowledged.

Name: **Dilbetigle Assefa**

Signature: _____

This thesis has been submitted for examination with my approve as university advisor.

Name: **A.K. Chaubay (Professor)**

Signature: _____

Addis Ababa university

July 2006